PEG-DAO showed bacteriostatic activity in a dose-dependent manner (Figure 1a). Different concentrations of D-Ala also demonstrated dose-dependent activity (Figure 1b). Bacteriostatic activity was not observed with treatment of PEG-DAO and L-Ala (Figure 1a). Adding 1 mg/mL catalase (5000–15,000 U/mL) to samples with PEG-DAO and D-Ala nullified the bacteriostatic activity of PEG-DAO (Figure 1c).

PEG-DAO restored antibacterial activity of NADPH oxidase-deficient mouse neutrophils

As H_2O_2 is a highly cell permeable oxidant, we examined H_2O_2 generated by PEG-DAO plus D-Ala in the medium to determine whether H_2O_2 could penetrate cell membranes and enter the cells. H_2O_2 treatment increased oxidative stress inside neutrophils, as shown by analysis using fluorescence flow cytometry in the presence of the fluorescent reactive oxygen species probe dichlorofluorescein diacetate (DCFH-DA) (Figure 2a). In the presence of 10 mmol/L D-Ala, treatment with PEG-DAO increased the intracellular H_2O_2 concentration in a dose-dependent manner as judged by this fluorescent probe (Figures 2b and c). However, PEG-DAO alone did not induce oxidative stress (data not shown). To mimic defective CGD neutrophils, mouse peritoneal neutrophils were treated with 10 μmol/L DPI to inhibit NADPH oxidase. DPI treatment increased the numbers of viable bacteria inside the treated neutrophils, as seen by the colony forming assay (Figure 2d). However, PEG-DAO treatment in the presence of 10 mmol/L D-Ala, restored bactericidal activity of DPI-treated defective neutrophils; the number of viable bacteria inside neutrophils almost recovered to the normal, non-CGD concentration. No enhancement of antibacterial activity by PEG-DAO in normal neutrophils was observed (Figure 2d).

PEG-DAO induced MPO-dependent bactericidal activity of CGD-equivalent mouse neutrophils

Consistent with the results shown in Figure 2, the bactericidal activity of mouse peritoneal neutrophils, which had been pretreated with DPI and thus had no NADPH oxidase activity, was restored by adding PEG-DAO and D-Ala (Figure 3). Treatment with 4-ABH, a specific inhibitor of MPO, clearly suppressed the bactericidal activity of normal mouse neutrophils. An interesting finding was the significant suppression of bactericidal activity of neutrophils by 4-ABH treatment, even with added PEG-DAO and D-Ala. This result demonstrates the important role of MPO in PEG-DAO-mediated bacterial killing (Figure 3).

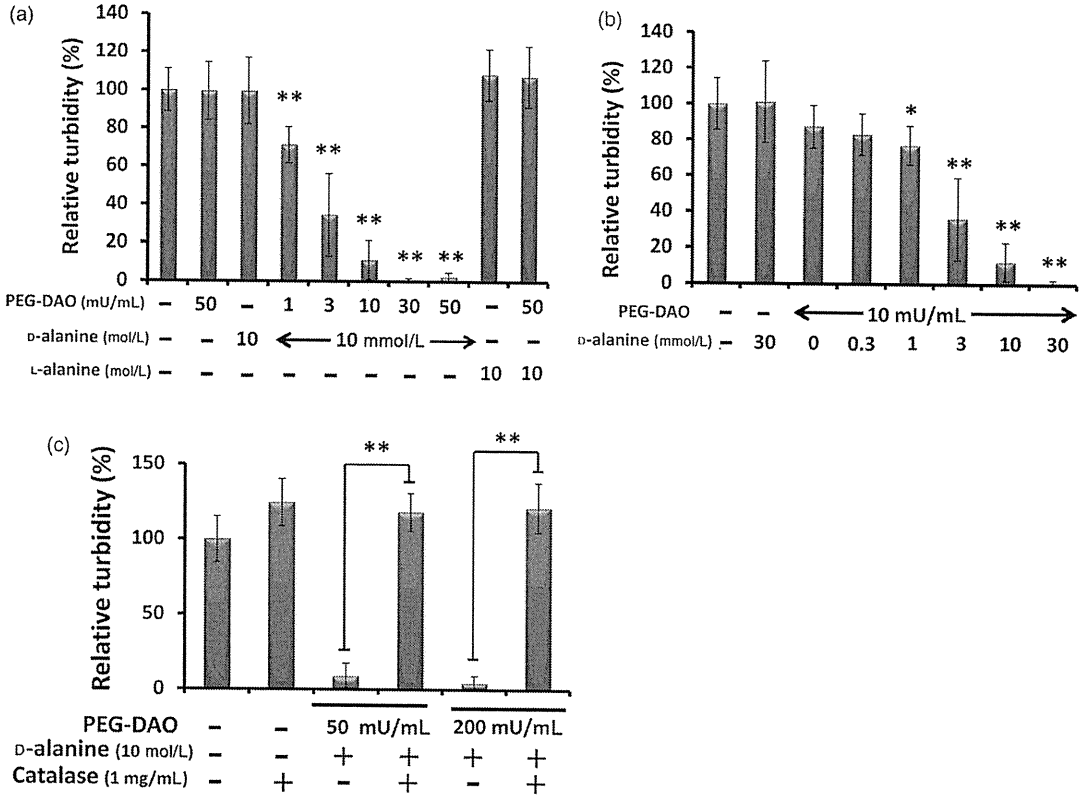

Figure 1 Bacteriostatic activity of polyethylene glycol-conjugated D-am-amino acid oxidase (PEG-DAO) against *Staphylococcus aureus*. (a) Increasing concentrations of PEG-DAO in the presence of 10 mmol/L D-Ala or (b) increasing concentrations of D-Ala in the presence of 10 mU/mL PEG-DAO were incubated with *S. aureus* bacteria (1×10^6 CFU/mL) for five hours, after which turbidity at 570 nm was measured. (c) *S. aureus* bacteria (1×10^6 CFU/mL) were incubated for five hours with PEG-DAO plus D-Ala with or without 1 mg/mL bovine catalase, and after which turbidity at 570 nm was measured. ** and * indicate statistically significant differences ($P < 0.01$) and ($P < 0.05$), respectively, by Student's *t*-test. Values are means ± SD ($n = 12$)

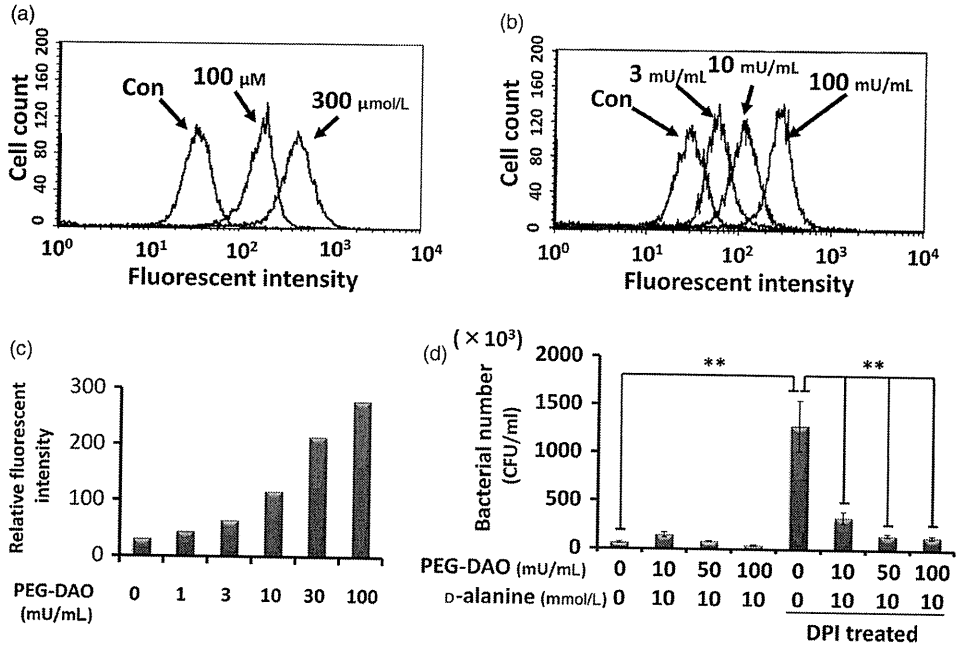

Figure 2 Increase in intracellular hydrogen peroxide (H_2O_2) by means of treatment with polyethylene glycol-conjugated D-amino acid oxidase (PEG-DAO) plus D-Ala and restoration of bactericidal activity of chronic granulomatous disease-like neutrophils. Mouse peritoneal neutrophils were pretreated with 10 μmol/L dichlorofluorescein diacetate, a fluorescent molecular probe for H_2O_2, and were then incubated with (a) increasing concentrations of H_2O_2 or (b) increasing concentrations of PEG-DAO (1–100 mU/mL) plus a fixed amount of 10 mmol/L D-Ala, followed by incubation for 30 min at room temperature. The fluorescence intensity of neutrophils was measured by means of a flow cytometer. (c) Normalized fluorescence intensity of cells in (b) representing intracellular reactive oxygen species. (d) Mouse peritoneal neutrophils were pretreated with 10 μmol/L diphenylene iodonium and were then incubated with opsonized *Staphylococcus aureus* to allow phagocytosis for 30 min. After removal of non-phagocytosed bacteria in the supernatant, neutrophils were treated with PEG-DAO plus 10 mmol/L D-Ala for 30 min. Viable bacteria inside the neutrophils were counted as described in Materials and methods. Values are means ± SD ($n = 4$). ** indicates statistically significant differences ($P < 0.01$) by Student's *t*-test

Restoration of bactericidal activity of human CGD neutrophils by PEG-DAO treatment

We examined the bactericidal activity of PEG-DAO with neutrophils from a patient with CGD, as they are known to have little antibacterial effect. We first checked the intracellular oxidant status before and after PEG-DAO treatment. In agreement with the results shown in Figure 2, treatment with PEG-DAO plus D-Ala increased the intracellular oxidative state (Figure 4a). CGDneutrophils showed less bactericidal activity as compared with healthy neutrophils. However, treatment with 10 or 30 mU/mL PEG-DAO restored the bactericidal activity of these CGD neutrophils to a considerable extent in the presence of 10 mmol/L D-Ala (Figure 4b).

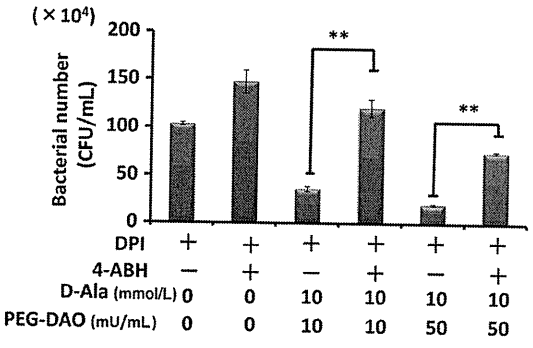

Figure 3 Polyethylene glycol-conjugated D-am-amino acid oxidase (PEG-DAO) restored the bactericidal activity of diphenylene iodonium-treated neutrophils, which depended on myeloperoxidase (MPO) activity. Mouse peritoneal neutrophils were treated with both DPI, an inhibitor of nicotinamide adenine dinucleotide phosphate oxidase, and 4-aminobenzoic acid hydrazide, an inhibitor of MPO. Cells were then incubated with opsonized *Staphylococcus aureus* to allow phagocytosis. After removal of non-phagocytosed bacteria, neutrophils were treated with PEG-DAO for 30 min. The number of viable bacteria was derived from the count of colonies on agar plates, as described in Materials and methods. Values are means ± SD ($n = 4$). ** indicates statistically significant differences ($P < 0.01$) by Student's *t*-test

Discussion

Patients with CGD have a genetic defect in NADPH oxidase, which results in deficient H_2O_2 generation and hence poor antimicrobial defense. Consequently, neutrophils from patients with CGD fail to kill bacteria, and chronic inflammation may result.[2,3] CGDneutrophils continue to evidence normal migration, phagocytosis and MPO enzyme activity; only their H_2O_2-generating capacity is severely impaired.[10] We thus hypothesized that supplementation with H_2O_2 would restore this function of CGD neutrophils.

H_2O_2 itself shows bactericidal activity *in vitro*, but intravenous injection of H_2O_2 does not result in antibacterial activity against bacteria *in vivo* because of the presence of excess catalase in systemic circulation.[11] In other words, circulating H_2O_2 *in vivo* is rapidly cleared by catalase, so no H_2O_2 is available for targeting to infected or inflamed

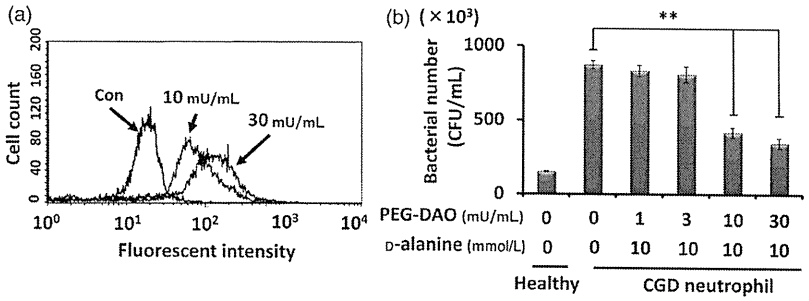

Figure 4 Restoration of bactericidal function of human chronic granulomatous disease (CGD) neutrophils by polyethylene glycol-conjugated D-am-amino acid oxidase (PEG-DAO) treatment. (a) Human CGD neutrophils were pretreated with 10 μmol/L dichlorofluorescein diacetate, an intracellular marker of oxystress, and were then incubated with PEG-DAO (10 or 30 mU/mL) and 10 mmol/L D-Ala for 30 min at room temperature. The fluorescence intensity of the neutrophils was measured by using a fluorescence flow cytometer. (b) CGD neutrophils were incubated with *Staphylococcus aureus* to allow phagocytosis. After removal of the non-phagocytosed *S. aureus* by centrifugation, neutrophils were treated with PEG-DAO and D-Ala for 30 min followed by incubation with 0.2% Tween-20 to liberate bacteria from the neutrophils. Serial dilutions of bacteria were then mixed with trypticase soy agar in Petri dishes and incubated overnight at 37°C, and bacterial colonies was counted. Values are means ± SD ($n = 3$). ** indicates statistically significant differences ($P < 0.01$) by Student's *t*-test

sites. Furthermore, H_2O_2 may harm mammalian cells that have no catalase or other antioxidants.[11] Thus, new strategies to deliver the H_2O_2 to the target site are required, which may provide a new strategy of H_2O_2-dependent treatment of infection and cancer.

To achieve the delivery of H_2O_2 to an infected or inflamed site, we prepared PEG-DAO, which retained a degree of H_2O_2-generating activity that was comparable with that of native DAO.[6,7] Also, DAO derived from a porcine source can be used in humans, because pegylation reduced the antigenicity of this enzyme. PEG-DAO accumulates preferentially in tumor tissue because of the EPR effect, the mechanism of which is based on the highly enhanced extravasation of macromolecules in the tumor and inflamed tissues. In addition, impaired lymphatic clearance of such macromolecules from interstitial space makes this effect more distinct. This increased vascular permeability is induced partly by overproduction of inflammatory vascular mediators such as bradykinin, nitric oxide and many others.[2,8]

The concentrations of D-amino acids, which are substrates of PEG-DAO, are extremely low in mammalian blood plasma, so H_2O_2 generation by PEG-DAO alone in systemic circulation is quite limited. However, we can induce H_2O_2 generation with an intravenous injection of D-amino acids. PEG-DAO at first accumulates predominantly at inflamed site because of the EPR effect. After several hours of PEG-DAO infusion via an intravenous route allowing PEG-DAO to accumulate more selectively at the disease site, at that time PEG-DAO concentration in blood is very low, D-amino acid is infused subsequently via the intravenous route. Thus, PEG-DAO is preferable for delivery of H_2O_2 to the inflamed sites or cancer tissue, and avoids systemic generation of H_2O_2.[6]

PEG-DAO plus D-Ala, as mediated by H_2O_2, showed bacteriostatic activity against *S. aureus* in a dose-dependent manner via production of H_2O_2 (Figure 1). These results indicate that PEG-DAO can serve as an antibacterial agent if it is selectively delivered to an infected site. This delivery became a possibility as a result of the prolonged plasma half-life of PEG-DAO and the EPR effect.

When PEG-DAO plus D-Ala was supplied to NADPH oxidase-deficient neutrophils, it increased the amount of H_2O_2 inside the cells (Figures 2 and 4). The fluorescent oxystress probe DCFH-DA, which effectively enters neutrophils, contains a diacetate group that is quickly hydrolyzed, so DCFH-DA becomes reactive to H_2O_2 and then fluorescent.[12] The higher fluorescence intensity of DCFH-DA thus indicates a higher oxidative state inside cells, but does not reflect the oxidative state outside cells. As expected, PEG-DAO treatment or H_2O_2 treatment increased the intracellular level of H_2O_2 in a dose-dependent manner (Figure 2a). Furthermore, in the presence of D-Ala, addition of PEG-DAO also increased the amount of intracellular H_2O_2 in a dose-dependent manner (Figures 2a and b). These results clearly indicate that PEG-DAO treatment can supply exogenous H_2O_2 efficiently to neutrophils and that this restored level of intracellular H_2O_2, as H_2O_2 is converted to the hypochlorite ion by MPO, would facilitate potent bactericidal activity of neutrophils from a CGD patient.

We also examined whether PEG-DAO treatment would restore the bactericidal activity of CGD-like neutrophils. We prepared these neutrophil mimics, which are similar to neutrophils in patients with CGD, by pretreatment with 10 μmol/L DPI, which achieves its effects by inhibiting NADPH oxidase and thus suppressing H_2O_2 generation.[13] In this experiment, we used PEG-DAO plus D-Ala and examined the effect of this treatment on phagocytosed bacteria. We observed a significant increase in the number of viable bacteria inside these neutrophils after DPI treatment (Figure 2d). In this setting, the bactericidal activity of DPI-treated neutrophils was similar to that of neutrophils from a CGD patient. However, PEG-DAO treatment of DPI-treated neutrophils greatly suppressed the number of viable bacteria inside neutrophils, almost to the number in healthy neutrophils (Figure 2d).

Most MPO exists in vacuoles in neutrophils,[14] and MPO oxidizes the chloride ion, with H_2O_2, to produce hypochlorous acid, one of the most potent bactericidal molecules in biological systems. We therefore hypothesized that restoration of bactericidal activity of DPI-treated neutrophils by treatment of PEG-DAO and D-Ala was mediated by the function of MPO. Consistent with our hypothesis, 4-ABH, an MPO inhibitor, suppressed the bactericidal activity of

the neutrophils, even in the treatment of PEG-DAO plus D-Ala (Figure 3).

As a more important result, we found that PEG-DAO plus D-Ala treatment restored the bactericidal activity of neutrophils from a CGD patient. Although the CGD neutrophils showed decreased bactericidal activity, in great contrast to healthy neutrophils (Figure 4), treatment with PEG-DAO plus D-Ala restored the bactericidal activity of these CGD neutrophils (Figure 4).

Our results thus demonstrated that H_2O_2 supplementation via PEG-DAO plus D-Ala would protect against bacterial infection. In our experiments, we used porcine DAO to prepare PEG-DAO. For porcine DAO, the K_{cat} and K_m values for D-proline are 43.3 s^{-1} and 2 mmol/L, respectively, whereas those corresponding values for D-Ala are 6.4 s^{-1} and 3.1 mmol/L.[15] Thus, using D-proline may be preferable to using D-Ala to treat CGD neutrophil, although this issue requires additional investigation. Furthermore, H_2O_2 can enter the cytosol of neutrophils and be converted to hypochlorous acid by MPO. These observations suggest that H_2O_2 supplementation via enzymatic action may become a plausible approach for treatment of patients with CGD. Less useful therapeutic strategies for CGD exist as yet, despite the great advances in the development of antimicrobial agents. The previously reported pharmacokinetics of PEG-DAO indicated an effective targeting ability to solid tumor as a result of the EPR effect. Bacterial components such as bacterial proteases and endotoxin facilitate the vascular permeability, and thus leakage of blood components such as albumin from circulating blood. Consequently, these macromolecules will accumulate at the infected or inflamed site.[16,17] Although accumulation property of macromolecular protein at the tumor and inflamed tissue is similar, accumulation of PEG-DAO at the inflamed tissue in CGD mouse model of human patients is yet to be determined. PEG-DAO pharmacokinetics may be similarly beneficial for targeting to the inflamed granuloma tissue in patients with CGD, although more studies are needed to confirm this possibility.

Author contributions: All authors participated in the design, interpretation of the studies and analysis of the data and review of the manuscript; HN conducted the experiments and wrote the manuscript with HM, TM and HN supplied the critical sample; JF and HM discussed the content constructively for the experiments and revised the manuscript.

ACKNOWLEDGEMENTS

The use of blood samples from a patient with CGD was approved by the Institutional Review Board of University of Miyazaki, Japan. This work was supported by Grant-in-Aid for Scientific Research 21791016 from the Ministry of Education, Culture, Sports, Science and Technology of Japan.

REFERENCES

1 Hohn DC, Lehrer RI. NADPH oxidase deficiency in X-linked chronic granulomatous disease. *J Clin Invest* 1975;**55**:707–13
2 Johnston RB Jr, Keele BB Jr, Misra HP, Lehmeyer JE, Webb LS, Baehner RL, rajagopalan KV. The role of superoxide anion generation in phagocytic bactericidal activity. Studies with normal and chronic granulomatous disease leukocytes. *J Clin Invest* 1975;**55**:1357–72
3 Repine JE, Clawson CC. Quantitative measurement of the bactericidal capability of neutrophils from patients and carriers of chronic granulomatous disease. *J Lab Clin Med* 1977;**90**:522–8
4 Burton K. The stabilization of D-amino acid oxidase by flavin-adenine dinucleotide, substrates and competitive inhibitors. *Biochem J* 1951;**48**:458–67
5 Mosebach KO. [Mechanism of action of some factors affecting D-amino acid oxidase. III. Reactions and significance of nascent hydrogen peroxides.]. *Hoppe Seylers Z Physiol Chem* 1957;**309**:206–18
6 Fang J, Sawa T, Akaike T, Maeda H. Tumor-targeted delivery of polyethylene glycol-conjugated D-amino acid oxidase for antitumor therapy via enzymatic generation of hydrogen peroxide. *Cancer Res* 2002;**62**:3138–43
7 Fang J, Deng D, Nakamura H, Akuta T, Qin H, Iyer AK, Greish K, Maeda H. Oxystress inducing antitumor therapeutics via tumor-targeted delivery of PEG-conjugated D-amino acid oxidase. *Int J Cancer J Int Cancer* 2008;**122**:1135–44
8 Matsumura Y, Maeda H. A new concept for macromolecular therapeutics in cancer chemotherapy: mechanism of tumoritropic accumulation of proteins and the antitumor agent smancs. *Cancer Res* 1986;**46**:6387–92
9 Fang J, Nakamura H, Maeda H. The EPR effect: unique features of tumor blood vessels for drug delivery, factors involved, and limitations and augmentation of the effect. *Adv Drug Deliv Rev* 2011;**63**:136–51
10 Gougerot-Pocidalo MA, Elbim C, Dang PM, El Benna J. [Primary immune deficiencies in neutrophil functioning]. *Presse Med* 2006;**35**:871–8
11 Shenep JL, Stokes DC, Hughes WT. Lack of antibacterial activity after intravenous hydrogen peroxide infusion in experimental Escherichia coli sepsis. *Infect Immun* 1985;**48**:607–10
12 Lebel CP, Bondy SC. Sensitive and rapid quantitation of oxygen reactive species formation in rat synaptosomes. *Neurochem Int* 1990;**17**:435–40
13 Ellis JA, Mayer SJ, Jones OT. The effect of the NADPH oxidase inhibitor diphenyleneiodonium on aerobic and anaerobic microbicidal activities of human neutrophils. *Biochem J* 1988;**251**:887–91
14 Rosen H, Crowley JR, Heinecke JW. Human neutrophils use the myeloperoxidase-hydrogen peroxide-chloride system to chlorinate but not nitrate bacterial proteins during phagocytosis. *J Biol Chem* 2002;**277**:30463–8
15 Molla G, Sacchi S, Bernasconi M, Pilone MS, Fukui K, Polegioni L. Characterization of human D-amino acid oxidase. *FEBS Lett* 2006;**580**:2358–64
16 Xing J, Moldobaeva N, Birukova AA. Atrial natriuretic peptide protects against *Staphylococcus aureus*-induced lung injury and endothelial barrier dysfunction. *J Appl Physiol* **110**:213–24 Q1
17 Kamata R, Yamamoto T, Matsumoto K, Maeda H. A serratial protease causes vascular permeability reaction by activation of the Hageman factor-dependent pathway in guinea pigs. *Infect Immun* 1985;**48**:747–53

(Received October 28, 2011, Accepted February 16, 2012)

ARTICLE IN PRESS
COREL-06300; No of Pages 7

Journal of Controlled Release xxx (2012) xxx–xxx

Contents lists available at SciVerse ScienceDirect

Journal of Controlled Release

journal homepage: www.elsevier.com/locate/jconrel

NANOMEDICINE

Review

Macromolecular therapeutics in cancer treatment: The EPR effect and beyond

Hiroshi Maeda

Institute of DDS Research, Sojo University, 4-22-1, Ikeda, Kumamoto, 860-0082, Japan

ARTICLE INFO

Article history:
Received 27 February 2012
Accepted 18 April 2012
Available online xxxx

Keywords:
EPR-effect
SMANCS
Tumor targeting
Heterogeneity of EPR effect
Augmentation of EPR effect
Vascular permeability

ABSTRACT

In this review, I have discussed various issues of the cancer drug targeting primarily related to the EPR (enhanced permeability and retention) effect, which utilized nanomedicine or macromolecular drugs. The content goes back to the development of the first polymer–protein conjugate anticancer agent SMANCS and development of the arterial infusion in Lipiodol formulation into the tumor feeding artery (hepatic artery for hepatoma). The brief account on the EPR effect and its definition, factors involved, heterogeneity, and various methods of augmentation of the EPR effect, which showed remarkably improved clinical outcomes are also discussed. Various obstacles involved in drug developments and commercialization are also discussed through my personal experience and recollections.

Contents

1. Introduction: from the past to the present

From the time of the hypothetical concept of the *magic bullet* proposed by Paul Ehrlich at the end of the 19th century, almost 40–50 years elapsed before the appearance of practical clinical drugs such as sulfonamide and penicillin for the control of microbial infections. However, more than 100 years have passed since Ehrlich's concept to achieve advances in cancer treatment. The field of cancer chemotherapy began when, in 1943 during World War II in Bari, Italy, nitrogen mustard gas, a chemical warfare agent, was accidentally found to have antileukemic activity. However, research aimed at discovering acceptable, effective anticancer agents has not achieved its goal. Only in the last 10 years have we developed promising agents such as imatinib (Glivec), which is quite effective against chronic myelogenous leukemia. Although SMANCS (discussed below)

E-mail address: hirmaeda@ph.sojo-u.ac.jp.

0168-3659/$ – see front matter © 2012 Elsevier B.V. All rights reserved.
doi:10.1016/j.jconrel.2012.04.038

Please cite this article as: H. Maeda, Macromolecular therapeutics in cancer treatment: The EPR effect and beyond, J. Control. Release (2012), doi:10.1016/j.jconrel.2012.04.038

was such a candidate, interest in it has been declining because of business reasons. Thus, antitumor drugs that would be effective against a wide range of solid tumors are not available, and ideal drugs that act against solid tumors do not yet exist. In fact, the overall cancer mortality rate has not changed very much in the past 50 years [1,2], whereas the mortality rate in patients with bacterial infections has dropped dramatically since antibiotics became available.

One of the fundamental difficulties in cancer therapy lies in the great genetic diversification seen in human cancers, even in individual patients in which the process of genetic alteration of patients' tumor would have progressed in the past 10–30 years by the time when the patient tumor was diagnosed. In the past 10–20 years, so-called molecular target drugs became popular as the least toxic but promising therapeutics. This trend, despite its being fashionable, is now rather problematic. In fact, these agents, such as the well-known example of molecular target drug, rofecoxib (Vioxx®, though it is not anticancer drug), with more than US$ 10 billion being paid as compensation for unexpected adverse effects, are not miracle drugs. The highly diverse genetic mutations in individual cancer patients, which were just mentioned, make the drug development strategy of utilizing a single molecular target, based on a tumor-specific molecular epitope or target enzyme, very difficult if not completely impossible [3–6].

Other concerns about molecular target anticancer agents include not only poor efficacy but also the cost of drugs to patients. Some drugs, for example, cost far more than interferon or other anticytokine agents. Many molecular target drugs for cancer cost almost US$ 10,000 per dose, or more than US$ 100,000 per year, yet the expected prolongation of life is a few weeks more than the expected survival time of 3 or 5 years for control subjects not receiving the drugs. One can find such information in various references [e.g., 7–12].

With regard to a new modality with potentially less cost, the drug-targeting method based on the enhanced permeability and retention (EPR) effect has a more universal application for solid tumors, so lower costs seem possible, with greater therapeutic effects on more types of tumors and fewer adverse effects. These reasons provide a good rationale for pursuing this method and encouraging such drug development. As this symposium issue will show, anticancer drugs that are more generally effective against solid tumors should be developed, and investigation of the EPR effect, which is based macromolecular therapeutics, will lead to ideal candidates. (Other examples, e.g., that of F. Kratz et al., will also appear in this special issue). Tables 1 and 2 summarize the definition of the EPR effect and the factors involved in solid tumors and inflammation.

One can, of course, argue that the heterogeneity of the EPR effect reduces its universal validity. The EPR effect is not perfect or effective for all solid tumors, because tumors of different patients vary greatly in actual clinical settings. For example, tumor diameters can be less than 1 cm to larger than 10 cm; and tumors can be highly hypoxic to normoxic, can have different pathological classes, are genetically diverse, can have partial or extensive necrosis, can have occluded or compressed vascular systems with or without blood coagulation in or around the tumor mass, and so on. This heterogeneity can be overcome in a number of ways. For instance, modulating the patient's hydrodynamic state by systemic (i.v.) infusion of angiotensin II leads to higher blood pressure on the laminar side and more effectively pushes a drug into the tumor interstitium. Section 3 in this article demonstrates the proof of this method in the clinical settings. We have also developed easier methods utilizing various vascular mediators, as given in Table 3.

Table 1
Profiles of the EPR effect.

Characteristics	Comments
Molecular size	Above 40 kDa; 800 kDa still shows an active EPR effect
Biocompatibility	No coagulation, no interaction with blood components and blood vessels, no cell lysis, no RES[a] clearance (e.g., macrophages). Protease bound protease-inhibitor is cleared in a few min even though biocompatible macromolecules.
Time required to achieve EPR effects	More than several hours in circulation in mice[b]. The trend can be seen even initial 30 min.
Drug retention time of macromolecular drugs in tumor	Mostly days to weeks[a], in great contrast to passive targeting of low MW drugs which is only few minutes[b].
pH (isoelectric point)/surface change	Weakly acidic to weakly cationic. Polycationic particles will disappear rapidly from circulation.

[a] Reticuloendothelial system, such as macrophages.
[b] Passive tumor targeting (visualization) can be observed by radiography with low MW contrast agents upon infusion into the artery. These images are visible for only a few minutes after the infusion, which is typical in passive targeting, but disappears in a few min. In contrast biocompatible nanomedicine exhibits prolonged tumor-retention period of days of weeks. Thus a great contrast to the passive targeting to the EPR effect.

Table 2
Factors and mediators involved in the EPR effect in cancer and inflammation, and their responsible enzymes or effectors.[a]

EPR effect-enhancing factors/ mediators	Enzymes responsible for factors	Comments: actions of enzymes and factors, or sources of factors
1. Bradykinin (kinin)	Kallikrein and other proteases, plasminogen activator produce bradykinin	Angiotensin I-converting enzyme (ACE) degrades kinin; ACE-inhibitor potentiates activity by blocking kinin degradation. Kinin induces NO synthase
2. Nitric oxide (NO)	Nitric oxide synthase (NOS), inducible isoform of NOS (iNOS)	Nitroglycerin, isosorbide dinitrate (ISDN, Nitrol®), and nitroprusside yield nitrate, and nitrite-reductase, which occurs in hypoxic tissue (tumor), generates NO in hypoxic tumors.
3. Prostaglandins (PGs)	Cyclooxygenase 2 (COX-2)	PGI_2 agonist/beraprost affect the EPR effect
4. Carbon monoxide (CO)	Heme oxygenase-1 (HO-1)	Hemin, NO, and ultraviolet light, and heat induce HO-1
5. Peroxynitrite ($ONOO^-$)	Generated by $NO + O_2^-$	Extremely rapid reaction
6. Matrix metalloproteinase (MMP), or collagenase (← proMMP)[b]	Procollagenase activation by $ONOO^-$	$ONOO^-$ activates pro-MMP[b] → MMP
7. Vascular endothelial growth factor (VEGF/VPF)	Nitric oxide synthase (NOS)	NO, endotoxin, and other cytokines can induce this VEGF
8. Tumor necrosis factor α (TNF-α) and TFG-β inhibitor	Cytokines, growth factor	Induces inflammation and normalization of tumor vasculature
9. Heat	Heat shock protein, HO-1 (HSP-32)	e.g. HO-1 and inflammation etc.

See text for detail.
[a] Above factors are most common mediators of inflammation and cancer that facilitate extravasation.
[b] proMMP: pro-matrix metalloproteinase (collagenase) is activated by $ONOO^-$ or by other proteases.

2. Our prototype polymer-conjugate drug, SMANCS, and a new strategy for intraarterial (i.a.) infusion: the ultimate tumor-targeted delivery

In 1979, we pioneered the development of the protein–polymer conjugate SMANCS, which is the antitumor protein drug neocarzinostatin (NCS) chemically conjugated with a synthetic copolymer of styrene–maleic acid copolymer (SMA) [13–15]. SMANCS exhibited unique properties compared with the parental NCS [14–18]. These properties included (i) prolongation of the plasma $t_{1/2}$ (by 20-fold); (ii) improved tumor-targeting capacity because of the EPR effect, i.e., a markedly

Please cite this article as: H. Maeda, Macromolecular therapeutics in cancer treatment: The EPR effect and beyond, J. Control. Release (2012), doi:10.1016/j.jconrel.2012.04.038

Table 3
Strategies to overcome the heterogeneity of the EPR effect, and augmentation of the EPR effect to enhance tumor drug delivery.[a]

Methods[a]	Mechanism	Remarks
1. Use of angiotensin II-induced hypertension	Hydrodynamic; vasoconstriction induced hypertension → mechanical opening of endothelial cell-cell gaps passively.	Drug is infused into the tumor-feeding artery via cathether.
2. Use of angiotensin I-converting enzyme (ACE) inhibitor such as enalapril	Selectively elevates the kinin level only in tumors, by inhibiting kinin degradation by ACE-inhibitor, which occurs in the tumor tissue.	Given orally, very safe, clinically proven.
3. Use of nitroglycerin given topically by dermal patch, or by infusion via the tumor-feeding artery	Generates NO in hypoxic tumor issue selectively. See analogy to angina pectoris.	Nitroglycerin, isosorbide dinitrate (ISDN, Nitrol®), nitroprusside, and others; clinically proven (see text).
4. Use of prostaglandin (PG) I_2 analogue, beraprost sodium	PG agonist effect (with the $t_{1/2}$ more than 100 times longer in plasma) when given orally.	
5. Use of TGF-β-inhibitor	TGF-β is tumor growth and differentiation factor. Facilitate productive of extracellular matrix. The inhibitor counteracts to restore vascular maturation and normalization, which may be affected by vascular mediator.	Shown effective in the pancreatic cancer in vivo model.
6. Use induction of HO-1, or a CO generator (ruthenium tri carbonyl, CORM2[b])	Zn protoporphyrin or hemin–polymer conjugates induce HO-1 in tumors; use of CORM2 generates CO. See text.	No data available for in vivo therapeutic efficacy.

[a] These strategies will be effective only with nanoparticle or polymeric drugs.
[b] Carbon monoxide-releasing molecule.

higher (10- to 20-fold) intratumor concentration compared with the concentration in plasma [15–21]; (iii) no immunogenicity [15]; and (iv) higher lipophilicity, which enabled solubilization and formulation with a lipid contrast agent (Lipiodol®) as a carrier (i.e., the SMANCS/Lipiodol formulation) [14,18,21–25]. This lipid formulation allowed truly selective tumor targeting and tumor delivery by infusion into the tumor-feeding artery via a catheter under X-ray guidance of angiographic technique as viewed on the monitoring screen [21–25]. A drug concentration in the tumor as much as 2000 times the concentration in blood (2000:1) can be achieved by using this method [22]. The EPR effect is now known to allow most macromolecular drugs to be selectively delivered to solid tumors, where they remain for very long periods, several weeks or months or even more [16,18,21–25]. This sustained drug activity will result in a marked therapeutic effect [18,22–24].

3. Advancements in tumor targeting with SMANCS/Lipiodol via the i.a. route

We have now extended the application of SMANCS/Lipiodol therapy, administered via i.a. infusion, to advanced, difficult-to-treat solid tumors such as massive and multiple metastatic liver cancers, bile duct carcinomas and cholangiocarcinomas, and pancreatic cancers and their metastatic nodules in the liver [24]. We also successfully treated massive renal cell cancer similarly, by infusion into the renal artery. Descriptions of these examples have been published [18,25]. In this article, we provide examples of such augmented drug delivery, by means of angiotensin II-induced high blood pressure, to advanced, difficult-to-treat tumors: pancreatic cancer with metastatic liver cancer (Fig. 1A and B), and metastatic liver cancer that had originated from gastric cancer, which had previously been removed (Fig. 1C and D).

For both cases, we infused SMANCS/Lipiodol i.a. under conditions of angiotensin II-induced high blood pressure (e.g., from 100 mm Hg to 150 mm Hg) [25]. The blood pressure of 150–160 mm Hg was achieved via slow i.v. infusion of 0.5 μg/ml angiotensin II, that is set in a 20 ml infusion syringe-pump. This method offers not only an improved therapeutic effect but also a diagnostic value, given the highly sensitive detection, by means of computed tomography (CT), of the tumor-selective uptake of Lipiodol, even in small tumor nodules with diameters of 3–5 mm. Another advantage of using angiotensin II-induced high blood pressure is application to more types of tumors that may be treated by this method. In fact almost all cases responded very well (25). Under normotension, as SMANCS/Lipiodol was originally used, the drug was most effective for primary liver cancer (hepatocellular carcinoma) but was less effective for metastatic liver cancer and cholangiocarcinoma. The reason for this difference may be poor drug delivery to the tumor because of the heterogeneity of the EPR effect. As Fig. 1 shows, the improved delivery method that utilizes angiotensin II-induced high blood pressure indeed makes SMANCS/Lipiodol highly effective. Another benefit of this method is the reduced time required for tumor regression (e.g., to achieve 50% of tumor volume), perhaps because of increased targeted drug delivery, and with less frequent drug administration needed.

4. Heterogeneity of the EPR effect, which hinders tumor delivery, and the method of circumventing this heterogeneous drug delivery [16–18]

Although the EPR effect offers the first step in the process of delivering drugs to tumor tissue or near tumor cells, solid tumors in clinical settings frequently have heterogeneous characteristics as described in Section 1, and some tumors impede drug access to tumors because of necrosis, fibrosis, clot formation, or interference by stromal tissue [16,17,26,27]. However, in the past several years, we have devised ways, by means of different techniques, to improve this process of drug delivery to such tumors, as described below and as shown in Table 3.

4.1. Induced hypertension by using a slow i.v. infusion of angiotensin II

Inducing hypertension via a slow i.v. infusion of angiotensin II [21,25,28,29] is more useful for macromolecular drugs and drug/Lipiodol formulations given during arterial infusion than for low-MW drugs. This method was briefly described above (Section 3). Low-MW drugs offer little advantage in this method, perhaps because of rapid diffusion or washout [29].

4.2. Using nitroglycerin or other nitric oxide (NO)-releasing agents

Nitroglycerin and other NO-releasing agents generate NO from NO_2^- selectively in hypoxic tumor tissue compared with normoxic tissues [30,31]. Thus, such nitro agents facilitate the EPR effect via local NO generation in tumors, with drug delivery enhanced 2- to 3-fold and an improved therapeutic effect. Yasuda et al. [32,33] and Siemens et al. [34] also demonstrated the beneficial effect of NO-releasing agents used in combination with conventional low-MW drugs. In this review, I describe clinical cases of bronchogenic lung cancer for which isosorbide dinitrate (ISDN), an NO-releasing agent, was administered 50–100 μg in 1–2 ml of physiological saline, bolus, via the bronchial artery immediately before SMANCS/Lipiodol infusion into the same bronchial artery (see Section 6).

4.3. Using an angiotensin-converting enzyme inhibitor (ACEI)

Solid tumors generate bradykinin, which would aid the EPR effect. ACEIs inhibit the degradation of bradykinin, thus raising the local bradykinin concentration in tumor tissue more than in other tissues in the body [16,17,26]. For example, use of the combination of an ACEI and hypertension improved monoclonal antibody delivery 2- to 3-fold

Please cite this article as: H. Maeda, Macromolecular therapeutics in cancer treatment: The EPR effect and beyond, J. Control. Release (2012), doi:10.1016/j.jconrel.2012.04.038

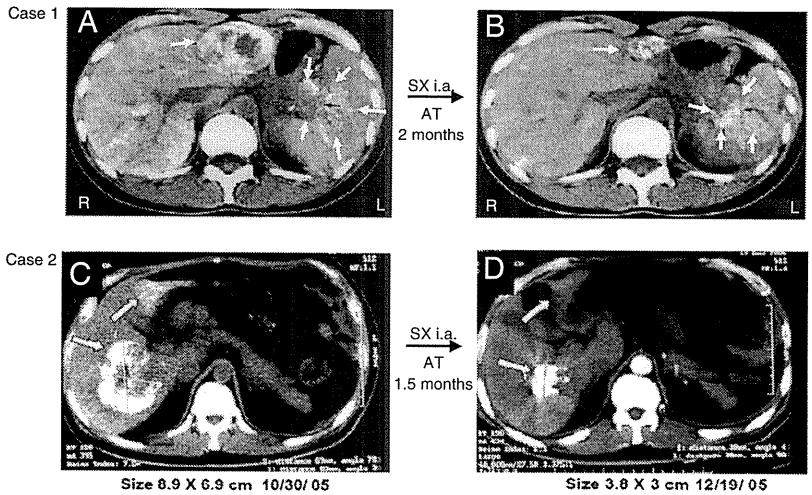

Fig. 1. Cases 1 and 2. Therapeutic effect of SMANCS/Lipiodol against advanced, difficult-to-treat cancers. The drug was infused via the tumor-feeding artery (hepatic artery) under angiotensin II-induced high blood pressure. A and C are abdominal CT scans 2 days after drug infusion. B and D are CT scans taken 2 and 1.5 months after drug infusion, respectively. Case 1. Pancreatic cancer with metastatic liver cancer (A) regressed significantly after 2 months. (B) Remarkable reduction in the size of the metastatic liver cancer (top, right). Case 2. Gastric cancer had metastasized to the liver (C). The two visible large tumor foci evidenced a marked size reduction after 1.5 months (D). White areas in the CT scans, other than bones, indicate where SMANCS/Lipiodol was selectively taken up by the tumors; other (normal) areas did not take up the drug (see the text for a description of the procedure). From Ref. [25].

in a xenograft mouse model of human gastric cancer [26,35]. This method was also validated effective by Dr. F. Kratz of Freiburg in different tumor model (personal communication).

4.4. Generating carbon monoxide (CO)

Fang et al. in our laboratory described the important role of heme oxygenase 1 (HO-1) in the EPR effect which is upregulated in most solid tumors; its product, CO, was also a factor influencing the EPR effect. CO has a physiological role similar to the vasodilator role of NO, so it will also have a key function in the EPR effect [36]. Thus, upregulation of HO-1 by HO-1 inducers such as pegylated hemin or similar agents, or CO-releasing agents (e.g., carbon monoxide-releasing molecule, CORM2), can facilitate the EPR effect [17,36].

5. Drug access to tumor cells and cellular drug uptake, followed by reaction of active drug with target molecules in tumor cells

Although nanoparticles can get to tumor tissues by means of the EPR effect, other issues complicating efficient drug uptake remain to be cleared. These issues include access of drugs to tumor cells and internalization of drugs, followed by release of the free or active drugs from macromolecular formulations composed of liposomes, micelles, or polymer conjugates such as polyethylene glycol (PEG), *N*-(2-hydroxyproply)methacrylamide (HPMA), or SMA. Achieving efficient drug uptake requires knowledge of tumor biology, such as targeting to unique receptors, making use of higher lipophilicity, and utilizing a unique ligand with high affinity to tumor cell receptors of a particular tumor. With regard to uptake of nanoparticle-drugs into tumor cells, in many cases cancer cells have more active endocytic uptake than do dormant normal cells.

Cellular drug uptake is more efficient with SMA micelles than with PEG-micelles [37 and our unpublished data]. For example, when we evaluated SMANCS and NCS, SMANCS was much more toxic to tumor cells than to normal cells [38]. Also, to kill 80% of the cells, NCS required more than 1 h at 30 nM, whereas SMANCS required only a few minutes at 15 nM [38]. Furthermore, a recent comparison of SMA-Zn protoporphyrin (PP) micelles and PEG–ZnPP micelles showed a more rapid cellular uptake for the former [37]. SMA–ZnPP micelles also demonstrated rapid uptake by tumor cells, with very quick disintegration of the micellar structure in the cells. Thus, release of free drug, ZnPP upon rapid endocytic uptake of SMA-ZnPP into tumor cells is anticipated [37]. Then, the free active drugs would be expected to react with target molecules in the cells (unpublished data).

6. Obstacles in drug development, drug promotion, and decision-making in business: dilemmas for science and business

6.1. Novel drug administration technique for use at the bedside

The first obstacle that we encountered in clinical drug development concerned the method of drug administration: the route via the tumor-feeding artery. In cardiology, the angiographic technique for imaging, which utilizes arterial infusion of a contrast agent to visualize an occluded artery and damaged tissue, is a routine practice in major hospitals. The same technique has been used much less frequently or very rarely in cancer treatment, although interventional radiologists utilize it, primarily for embolization of the tumor-feeding artery so as to achieve tumor necrosis, with limited effects [39].

In SMANCS/Lipiodol therapy, the lipid formulation of SMANCS is infused into the tumor-feeding artery—the hepatic artery for hepatoma, the renal artery for cancer of the kidney, and the bronchial artery for lung cancer or bronchogenic cancer (Figs. 1–3) [18,23,25]. This infusion occurs simultaneously with angiographic imaging of the tumor, with identification of the tumor-feeding artery. This technique requires adequate skill to manipulate the catheter under X-ray guidance, more skill than that needed for the commonly used i.v. infusion, and not every health care professional can perform such drug administration. Also, some pharmaceutical companies do not view such an elaborate method favorably, so it becomes a negative incentive for a business undertaking. However, this perception may be reversed when members of top management of a company carefully examine and investigate the positive clinical outcomes. For example, organizing a task force to promote this therapeutic modality using SMANCS/Lipiodol may encourage opening of a new market.

6.2. Market size: n×T dominates the corporate decision

The second obstacle to developing new candidate drugs, which is usually the first question that people ask us, is, how big will the market

Please cite this article as: H. Maeda, Macromolecular therapeutics in cancer treatment: The EPR effect and beyond, J. Control. Release (2012), doi:10.1016/j.jconrel.2012.04.038

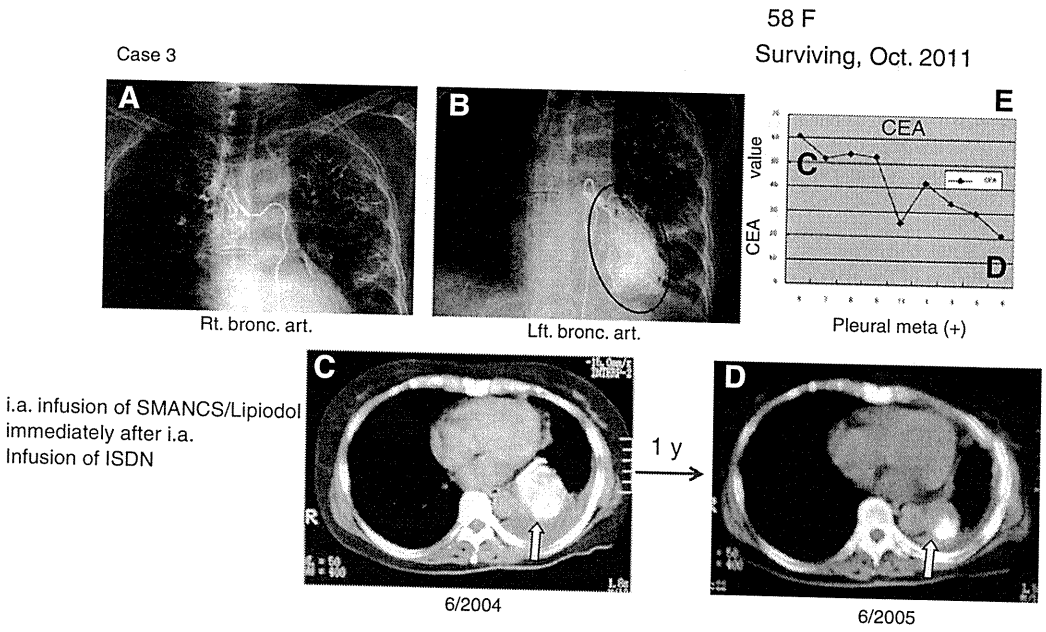

Fig. 2. Case 3. Lung cancer (adenocarcinoma). A and B are angiograms showing infusion of contrast agent into the right bronchial artery (A) and left bronchial artery (B). These X-ray images indicate that the tumor is fed by two different arteries. (C) Initial CT scan at the start of treatment (arrow shows tumor area). (D) CT scan showing considerable tumor regression (arrow) after 1 year. SMANCS/Lipiodol, about 0.5 ml (mg), was infused into each bronchial artery immediately after infusion of a microdose of Nitrol (10–50 μg/dose). (D) One year after treatment, the tumor in the pleural cavity is considerably smaller. White areas indicate remaining drug. (E) Graph showing the decrease in the tumor marker CEA (carcinoembryonic antigen); C and D in [E] correspond to the CT scans in C and D.

be? When we began the clinical application of SMANCS/Lipiodol to treat hepatoma in Japan in the 1980s, about 20,000 cases occurred per year, which by 2010 had increased to about 33,000. In the United States, the corresponding number in the 1980s was about 10,000, although it is much larger now, which was not a favorable size for drug development. In addition, not all of 10,000 patients would be using SMANCS so that actual market size would be far smaller.

Today in Japan, almost 500,000 new cancer cases arise annually. However, in contrast to the number of cancer patients, the number of patients in Japan with diabetes mellitus, hypertension, hypercholesterolemia, and osteoporosis, which are the primarily chronic diseases, exceeds several million. In addition, cancer patients require a much shorter period of drug administration compared with patients with those chronic diseases. Therefore, for anticancer drugs, the product of n (number of patients

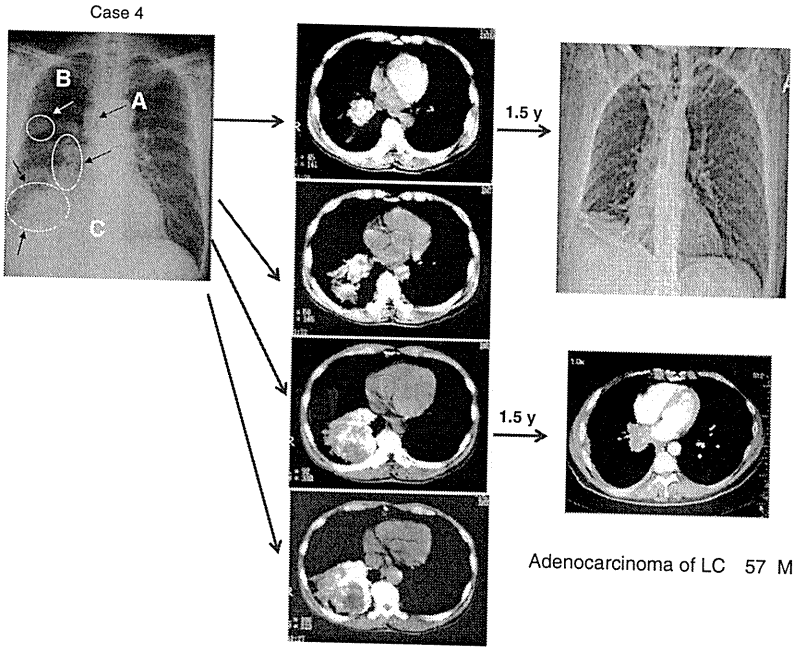

Fig. 3. Case 4. Lung adenocarcinoma. (Top left) Initial chest X-ray showing multiple tumors A, B, and C (circled areas, arrows). The patient underwent Nitrol infusion followed by SMANCS/Lipiodol infusion of 0.5 mg/0.5 ml into both bronchial arteries, as in Case 3. (Middle) CT scans from the subscapular to the lower pleural cavity at the time of initial infusion. (Right) Both chest X-ray (top) and CT scan (bottom) show remarkable tumor regression after 1.5 years; and the patient had no subjective complaints during this period.

Please cite this article as: H. Maeda, Macromolecular therapeutics in cancer treatment: The EPR effect and beyond, J. Control. Release (2012), doi:10.1016/j.jconrel.2012.04.038

eligible to use a drug for the approved tumor type) × T (time period during which the drug will be used) is far less than that for antihypertensive drugs, for instance. Furthermore, for any anticancer drug, a regulatory agency will approve its use by clinicians for only a specific type of cancer, e.g., brain, esophageal, pancreatic, or bile duct cancer individually, and its use for other types of cancer is not permitted. If a clinician in Japan prescribes the drug for another, unapproved type of cancer, the national insurance will not cover any related medical expenses, so that the patient must pay all medical expenses. In other words, use of a drug for an unapproved disease is not permitted—no off-label drug use is allowed in Japan. Therefore, in view of the 10,000–20,000 patients per year with many of these types of cancer in Japan, i.e., not much more than 50,000 patients per year, the market size (n × T), may be about 1/1000–1/10,000 for each cancer type, compared with, for example, that for statins (anticholesterol agents). Antihypercholesterolemic drugs, for instance, were obviously more lucrative because several million patients would use them for far longer than, say, 10–20 years. Many large pharmaceutical companies are therefore less enthusiastic about getting involved in anticancer drug development, which for them is not a high priority. A market size of half-a-million may be moderately interesting. A related issue concerns development of drugs for childhood cancer, in which there is not much interest. The development of orphan drugs also lags behind need, so society needs some system to support orphan drug development as well in Japan and elsewhere.

When SMANCS/Lipiodol was first demonstrated to be very effective against liver cancer, the market size in the United States was small, about 10,000, and the potential market for this drug was not so lucrative. The company that was developing SMANCS/Lipiodol in Japan also did little to promote the drug, regardless of its advantages—remarkable clinical benefits and very few adverse effects. Such decisions depend on the policies of each individual pharmaceutical company, and unfortunately, the executives of the company developing SMANCS/Lipiodol did not see the potential impact of this drug in Japan or elsewhere. In addition, this therapeutic strategy, which would have stimulated a paradigm change in solid tumor treatment as described earlier herein, would have stimulated the growth of a new market for use of this agent to treat other solid cancers.

With regard to the cost/benefit issue for cancer patients, many conventional anticancer drugs usually produce severe side effects but have marginal therapeutic efficacy and high costs. High drug prices mean that the drugs will be highly profitable and lucrative for the pharmaceutical companies. SMANCS/Lipiodol, however, is usually administered three to five times in the first year, and then two or three times the next year. This administration schedule means that the number of sales is quite small, which thus impedes drug development.

We have discovered very interesting therapeutic drugs or new modalities for treatment of cancer and other rare diseases [39–42], but making such drugs or modalities available for patients with chronic granulomatous disease [41] or fulminant hepatitis with hyperbilirubinemia [43] requires enthusiastic physicians, pharmaceutical scientists, and industrialists. In practice, development of such drugs is indeed quite difficult or almost, if not completely, impossible.

6.3. Regulation in drug development

The third obstacle to developing new drugs concerns regulatory agencies. SMANCS consists of two parts: NCS (protein) and a synthetic copolymer of SMA. Both parts are chemically conjugated, so the drug is a single chemical entity. For its administration, we developed a new formulation with the lipid contrast agent Lipiodol, as described above. However, a regulatory agency in Europe required all data related to toxicity, pharmacokinetics, and pharmacodynamics, as well as clinical data, to be provided separately for each component: NCS, Lipiodol, and SMA copolymer, (the latter two have no cytotoxic or anticancer activity). Our preclinical data in rodents showed that only the SMANCS in Lipiodol formulation demonstrated the far greater therapeutic benefit as well as diagnostic value. If a company had carried out such experiments for each separate component in humans, the cost would have been prohibitory, so no such experiments were done. In addition, my colleague physicians, with no reason to believe that clinical benefit would ensue, objected to doing such unethical clinical studies of humans, with legal actions following as the worst outcome.

Therefore, during the filing for approval process, regulatory agencies should require and examine only preclinical and clinical data of the drug being used. The agencies should be concerned with the formulation of the drug as used in the clinical setting, not each separate component. To conduct experiments that are not directly relevant to clinical practice or patient benefit will delay drug development and create great financial burdens on companies and society. In fact, cost reduction in drug development is now becoming a critical issue. Not only in the United States but also in Japan and Europe, huge national financial debts are causing difficulties, and medical expenditure is indeed partly responsible for this; reduction in medical cost is thus a requirement in every aspect of medical care, including drug development [7–10,44]. Therefore, imposing unreasonable requirements for filing for drug approval should be avoided [7,8].

7. Conclusion

In this article, I describe my personal experiences with the EPR effect and development of macromolecular therapeutics (SMANCS), including marketing issues. Essential focal points of development of such drugs involve the cost of the drug and its efficacy. Price setting is a complex issue: if a price is too low, a company will lose interest, but if it is too high, society will suffer. Furthermore, in the current arena of anticancer drug development, the need for a wide range of knowledge about cancer genomics and cancer biology is not fully appreciated. Drug development based on the EPR effect is certainly an important first step, but some problems still remain. Even after a drug is delivered to cancer tissue, it must be taken up by tumor cells, and free active drug must then be released and interact with target molecules. The case of SMA–ZnPP micelles serves as an example of such a drug in development. Also, the heterogeneity of the EPR effect must be overcome. I have addressed this heterogeneity and achieved realistic in vivo solutions that have no obvious adverse effects, and I will be excited when clinicians adopt these solutions. The enthusiasm of scientists as well as industry is by far the most important key for successful drug development.

I also discuss how regulatory agencies should act responsibly, with prudence and wisdom, not only with regard to safety issues, even when the remotest possibility of any harm may exist, but also with regard to economic burdens to society at large. Clinical efficacy is, of course, the most important issue, and in addition, patients should display a high degree of satisfaction with their treatment.

Acknowledgments

I am most grateful to Drs. A. Nagamitsu and K. Greish for permitting me to use unpublished Figs. 2 and 3. I also thank all my previous and present colleagues for their collaboration Ms. J.B. Gandy for editing, and Ms. A. Takaki for secretarial support.

References

[1] C. Leaf, Why we're losing the war on cancer, Fortune 149 (2004) 76–97.
[2] G.L. Gabor Miklos, The human cancer genome project—one more misstep in the war on cancer, Nat. Biotechnol. 23 (2005) 535–537.
[3] L.D. Wood, D.W. Parsons, S. Jones, J. Lin, T. Sjöblom, R.J. Leary, D. Shen, S.M. Boca, T. Barber, J. Ptak, N. Silliman, S. Szabo, Z. Dezso, V. Ustyanksky, T. Nikolskaya, Y. Nikolsky, R. Karchin, P.A. Wilson, J.S. Kaminker, Z. Zhang, R. Croshaw, J. Willis, D. Dawson, M. Shipitsin, J.K. Willson, S. Sukumar, K. Polyak, B.H. Park, C.L. Pethiyagoda, P.V. Pant, D.G. Ballinger, A.B. Sparks, J. Hartigan, D.R. Smith, E. Suh, N. Papadopoulos, P. Buckhaults, S.D. Markowitz, G. Parmigiani, K.W. Kinzler, V.E. Velculescu, B. Vogelstein, The genomic landscapes of human breast and colorectal cancers, Science 318 (2007) 1108–1113.

Please cite this article as: H. Maeda, Macromolecular therapeutics in cancer treatment: The EPR effect and beyond, J. Control. Release (2012), doi:10.1016/j.jconrel.2012.04.038

[4] T. Sjöblom, S. Jones, L.D. Wood, D.W. Parsons, J. Lin, T.D. Barber, D. Mandelker, R.J. Leary, J. Ptak, N. Silliman, S. Szabo, P. Buckhaults, C. Farrell, P. Meeh, S.D. Markowitz, J. Willis, D. Dawson, J.K. Willson, A.F. Gazdar, J. Hartigan, L. Wu, C. Liu, G. Parmigiani, B.H. Park, K.E. Bachman, N. Papadopoulos, B. Vogelstein, K.W. Kinzler, V.E. Velculescu, The consensus coding sequences of human breast and colorectal cancers, Science 314 (2006) 268–274.
[5] R. Mayer, Targeted therapy for advanced colorectal cancer—more is not always better, N. Engl. J. Med. 360 (2009) 623–625.
[6] S.P. Shah, R.D. Morin, J. Khattra, L. Prentice, T. Pugh, A. Burleigh, A. Delaney, K. Gelmon, R. Guliany, J. Senz, C. Steidl, R.A. Holt, S. Jones, M. Sun, G. Leung, R. Moore, T. Severson, G.A. Taylor, A.E. Teschendorff, K. Tse, G. Turashvili, R. Varhol, R.L. Warren, P. Watson, Y. Zhao, C. Caldas, D. Huntsman, M. Hirst, M.A. Marra, S. Aparicio, Mutation evolution in a lobular breast tumor profiled at single nucleotide resolution, Nature 461 (2009) 809–813.
[7] Anonymous, Editorial, Welcome clinical leadership at NICE, Lancet 372 (2008) 601.
[8] Story from BBC News, Liver cancer drug 'too expensive', http://news.bbc.co.uk/2/hi/health/8367614.stm.
[9] K. Baicker, M.E. Chernew, The economics of financing Medicare, N. Engl. J. Med. 365 (4) (2011) e7.
[10] T. Fojo, C. Grady, How much is life worth: cetuximab, non-small cell lung cancer, and the $440 billion question, J. Natl. Cancer Inst. 101 (2009) 1044–1048.
[11] W.J. Chng, L.A. Loeb, J.H. Bielas, Limits to the human cancer genome project? Science 315 (2007) 762–764.
[12] J. Tol, M. Koopman, A. Cats, C.J. Rodenburg, G.J. Creemers, J.G. Schrama, F.L. Erdkamp, A.H. Vos, C.J. van Groeningen, H.A. Sinnige, D.J. Richel, E.E. Voest, J.R. Dijkstra, M.E. Vink-Börger, N.F. Antonini, L. Mol, J.H. van Krieken, O. Dalesio, C.J. Punt, Chemotherapy, bevacizumab, and cetuximab in metastatic colorectal cancer, N. Engl. J. Med. 360 (2009) 563–572.
[13] H. Maeda, J. Takeshita, R. Kanamaru, A lipophilic derivative of neocarzinostatin: a polymer conjugation of an antitumor protein antibiotic, Int. J. Pept. Protein Res. 14 (1979) 81–87.
[14] H. Maeda, M. Ueda, T. Morinaga, T. Matsumoto, Conjugation of poly(styrene-co-maleic acid) derivatives to the antitumor protein neocarzinostatin: pronounced improvements in pharmacological properties, J. Med. Chem. 28 (1985) 455–461.
[15] H. Maeda, T. Matsumoto, T. Konno, K. Iwaki, M. Ueda, Tailor-making of protein drugs by polymer conjugation for tumor targeting: a brief review on Smancs, J. Protein Chem. 3 (1984) 181–193.
[16] H. Maeda, Tumor-selective delivery of macromolecular drugs via the EPR effect: background and future prospects, Bioconjug. Chem. 21 (2010) 797–802.
[17] J. Fang, H. Nakamura, H. Maeda, EPR effect: the unique characteristics of tumor blood vessels for drug delivery, factors involved, its limitation and augmentation, Adv. Drug Deliv. Rev. 63 (2011) 136–151.
[18] H. Maeda, Enhanced permeability and retention effect in relation to tumor targeting, in: F. Kratz, P. Senter, H. Steinhagen (Eds.), Drug Delivery in Oncology. From Basic Research to Cancer Therapy, Wiley-VCH Verlag GmbH & Co. KG, Weinheim, Germany, 2011, pp. 65–84.
[19] K. Hochdörffer, G.D. Stefano, H. Maeda, F. Kratz, Liver tumor targeting, in: F. Kratz, P. Senter, H. Steinhagen (Eds.), Drug Delivery in Oncology. From Basic Research to Cancer Therapy, Wiley-VCH Verlag GmbH & Co. KG, Weinheim, Germany, 2011, pp. 1519–1568.
[20] Y. Matsumura, H. Maeda, A new concept for macromolecular therapeutics in cancer chemotherapy: mechanism of tumoritropic accumulation of proteins and the antitumor agent SMANCS, Cancer Res. 46 (1986) 6387–6392.
[21] H. Maeda, T. Sawa, T. Konno, Mechanism of tumor-targeted delivery of macromolecular drugs, including the EPR effect in solid tumor and clinical overview of the prototype polymeric drug SMANCS, J. Control. Release 74 (2001) 47–61.
[22] K. Iwai, H. Maeda, T. Konno, Use of oily contrast medium for selective drug targeting to tumor: enhanced therapeutic effect and X-ray image, Cancer Res. 44 (1984) 2115–2121.
[23] T. Konno, H. Maeda, K. Iwai, S. Maki, S. Tashiro, M. Uchida, Y. Miyauchi, Selective targeting of anti-cancer drug and simultaneous image enhancement in solid tumors by arterially administered lipid contrast medium, Cancer 54 (1984) 2367–2374.
[24] S. Maki, T. Konno, H. Maeda, Image enhancement in computerized tomography for sensitive diagnosis of liver cancer and semiquantitation of tumor selective drug targeting with oily contrast medium, Cancer 56 (1985) 751–757.
[25] A. Nagamitsu, K. Greish, H. Maeda, Elevating blood pressure as a strategy to increase tumor targeted delivery of macromolecular drug SMANCS: cases of advanced solid tumors, Jpn. J. Clin. Oncol. 39 (2009) 756–766.
[26] H. Maeda, Vascular permeability in cancer and infection as related to macromolecular drug delivery, with emphasis on the EPR effect for tumor-selective drug targeting, Proc. Jpn. Academy, Series B. 88 (2012) 53–71.
[27] J. Daruwalla, M. Nikfarjam, K. Greish, C. Malcontenti-Wilson, V. Muralidharan, C. Christophi, H. Maeda, In vitro and in vivo evaluation of tumor targeting SMA–pirarubicin micelles: survival improvement and inhibition of liver metastases, Cancer Sci. 101 (2010) 1866–1874.
[28] M. Suzuki, K. Hori, I. Abe, S. Saito, H. Sato, A new approach to cancer chemotherapy: selective enhancement of tumor blood flow with angiotensin II, J. Natl. Cancer Inst. 67 (1981) 663–669.
[29] C.J. Li, Y. Miyamoto, Y. Kojima, H. Maeda, Augmentation of tumour delivery of macromolecular drugs with reduced bone marrow delivery by elevating blood pressure, Br. J. Cancer 67 (1993) 975–980.
[30] H. Maeda, Nitroglycerin enhances vascular blood flow and drug delivery in hypoxic tumor tissues: analogy between angina pectoris and solid tumors and enhancement of the EPR effect, J. Control. Release 142 (2010) 296–298.
[31] T. Seki, J. Fang, H. Maeda, Enhanced delivery of macromolecular antitumor drugs to tumors by nitroglycerin application, Cancer Sci. 100 (2009) 2426–2430.
[32] H. Yasuda, M. Yamaya, K. Nakayama, T. Sasaki, S. Ebihara, A. Kanda, M. Asada, D. Inoue, T. Suzuki, T. Okazaki, H. Takahashi, M. Yoshida, T. Kaneta, K. Ishizawa, S. Yamanda, N. Tomita, M. Yamasaki, A. Kikuchi, H. Kubo, H. Sasaki, Randomized phase II trial comparing nitroglycerin plus vinorelbine and cisplatin with vinorelbine and cisplatin alone in previously untreated stage IIIB/IV non-small cell lung cancer, J. Clin. Oncol. 24 (2006) 688–694.
[33] H. Yasuda, K. Nakayama, M. Watanabe, S. Suzuki, H. Fuji, S. Okinaga, A. Kanda, K. Zayazu, T. Sasaki, M. Asada, T. Suzuki, M. Yoshida, S. Yamanda, D. Inoue, T. Kaneta, T. Kondo, Y. Takai, H. Sasaki, K. Yanagihara, M. Yamaya, Nitroglycerin treatment may increase response to docetaxel and carboplatin regimen via inhibitions of hypoxia-inducible factor-1 pathway and P-glycoprotein in patients with lung adenocarcinoma, Clin. Cancer Res. 12 (2006) 6748–6757.
[34] D.R. Siemens, J.P.W. Heaton, M.A. Adams, J. Kawakami, C.H. Graham, Phase II study of nitric oxide donor for men with increasing prostate-specific antigen level after surgery or radiotherapy for prostate cancer, Urology 74 (2009) 878–883.
[35] A. Noguchi, T. Takahashi, T. Yamaguchi, K. Kitamura, A. Noguchi, H. Tsurumi, K. Takashina, H. Maeda, Enhanced tumor localization of monoclonal antibody by treatment with kininase II inhibitor and angiotensin II, Jpn. J. Cancer Res. 83 (1992) 240–243.
[36] J. Fang, H. Qin, H. Nakamura, K. Tsukigawa, H. Maeda, Carbon monoxide, generated by heme oxygenase-1, mediates the enhanced permeability and retention (EPR) effect of solid tumor, Cancer Sci. 102 (2012) 535–541.
[37] H. Nakamura, J. Fang, B. Gahininath, K. Tsukigawa, H. Maeda, Intracellular uptake and behavior of two types zinc protoporphyrin (ZnPP) micelles, SMA–ZnPP and PEG–ZnPP as anticancer agents; unique intracellular disintegration of SMA micelles, J. Control. Release 155 (2011) 367–375.
[38] T. Oda, F. Sato, H. Yamamoto, M. Akagi, H. Maeda, Cytotoxicity of smancs in comparison with other anticancer agents against various cells in culture, Anticancer Res. 9 (1989) 261–266.
[39] R. Avtister, J. Wallace, Interventional radiology for the cancer patient, in: W.K. Hong, R.C. Bast, W.N. Hait, D.W. Kufe, R.E. Pollock, R.R. Weichelbaum; J.F. Holland, E. Frei (Eds.), Holland-Frei Cancer Medicine, 8th edition, People's Medical Publishing House—USA, Shelton, CT, 2010, pp. 490–497.
[40] T. Sawa, J. Wu, T. Akaike, H. Maeda, Tumor-targeting chemotherapy by a xanthine oxidase–polymer conjugate that generates oxygen-free radicals in tumor tissue, Cancer Res. 60 (2000) 666–671.
[41] J. Fang, H. Qin, T. Seki, H. Nakamura, K. Tsukigawa, H. Maeda, Therapeutic potential of pegylated hemin for ROS-related diseases via induction of heme oxygenase-1: results from a rat hepatic ischemia/reperfusion injury model, J. Pharmacol. Exp. Ther. 339 (2011) 779–789.
[42] H. Nakamura, J. Fang, H. Maeda, Protective role of D-amino acid oxidase against bacterial infection, Infect. Immun. 80 (2012) 1546–1553.
[43] M. Kimura, Y. Matsumura, Y. Miyauchi, H. Maeda, A new tactic for the treatment of jaundice: an injectable polymer-conjugated bilirubin oxidase, Proc. Soc. Exp. Biol. Med. 188 (1988) 364–369.
[44] P.B. Ginsburg, C. White, Health care's role in deficit reduction — guiding principles, N. Engl. J. Med. 365 (2011) 1559–1561.

Please cite this article as: H. Maeda, Macromolecular therapeutics in cancer treatment: The EPR effect and beyond, J. Control. Release (2012), doi:10.1016/j.jconrel.2012.04.038

European Journal of Pharmaceutics and Biopharmaceutics xxx (2012) xxx–xxx

Contents lists available at SciVerse ScienceDirect

European Journal of Pharmaceutics and Biopharmaceutics

journal homepage: www.elsevier.com/locate/ejpb

Research paper

HSP32 (HO-1) inhibitor, copoly(styrene-maleic acid)-zinc protoporphyrin IX, a water-soluble micelle as anticancer agent: In vitro and in vivo anticancer effect ☆

Jun Fang [a,b,1], Khaled Greish [a,c,1], Haibo Qin [a,b,d], Long Liao [a,b,d], Hideaki Nakamura [a,b], Motohiro Takeya [e], Hiroshi Maeda [a,b,*]

[a] Laboratory of Microbiology and Oncology, Faculty of Pharmaceutical Sciences, Sojo University, Kumamoto, Japan
[b] DDS Research Institute, Sojo University, Kumamoto, Japan
[c] Department of Pharmacology and Toxicology, University of Otago, Dunedin, New Zealand
[d] Department of Applied Microbial Technology, Sojo University, Kumamoto, Japan
[e] Department of Pathology, Kumamoto University Medical School, Kumamoto, Japan

ARTICLE INFO

Article history:
Received 27 October 2011
Accepted in revised form 21 April 2012
Available online xxxx

Keywords:
HSP32
Heme oxygenase-1
EPR effect
Styrene-maleic acid copolymer
Cancer chemotherapy
Zinc protoporphyrin

ABSTRACT

We reported previously the antitumor effect of heme oxygenase-1 (HO-1) inhibition by zinc protoporphyrin IX (ZnPP). ZnPP per se is poorly water soluble and thus cannot be used as anticancer chemotherapeutic. Subsequently, we developed water-soluble micelles of ZnPP using styrene-maleic acid copolymer (SMA), which encapsulated ZnPP (SMA–ZnPP). In this report, the in vitro and in vivo therapeutic effects of SMA–ZnPP are described. In vitro experiments using 11 cultured tumor cell lines and six normal cell lines revealed a remarkable cytotoxicity of SMA–ZnPP against various tumor cells; average IC_{50} is about 11.1 μM, whereas the IC_{50} to various normal cells is significantly higher, that is, more than 50 μM. In the pharmacokinetic study, we found that SMA–ZnPP predominantly accumulated in the liver tissue after i.v. injection, suggesting its applicability for liver cancer. As expected, a remarkable antitumor effect was achieved in the VX-2 tumor model in the liver of rabbit that is known as one the most difficult tumor models to cure. Antitumor effect was also observed in murine tumor xenograft, that is, B16 melanoma and Meth A fibrosarcoma. Meanwhile, no apparent side effects were found even at the dose of ~7 times higher concentration of therapeutics dose. These findings suggest a potential of SMA–ZnPP as a tool for anticancer therapy toward clinical development, whereas further investigations are warranted.

1. Introduction

Zinc protoporphyrin IX (ZnPP) is a member of metalloporphyrins in which the heme iron is replaced by zinc, which becomes a competitive inhibitor of heme oxygenase (HO). HO is the key enzyme in the degradation of heme and exhibits antioxidative and antiapoptotic effects [1,2]. HO-1 is also a member of heat shock protein (HSP) family, namely HSP32 [2,3]. HO-1 is the inducible isoform of HO as a result of various intracellular and extracelluar stimuli, such as oxystress including superoxide radical, UV irradiation, nitric oxide and hypoxia [2–6]. Subsequently, its critical role in protecting cells against such insults has been reported [2–6].

High expression of HO-1 is now well known in many solid tumors [2,5,6], which is at least partly associated with the hypoxic micro-environment that is common in most solid tumors. Moreover, it is interesting that many cancer cells lost or downregulate antioxidative enzymes such as catalase, superoxide dismutase and glutathione peroxidase [7–11]. HO-1 thus serves as an essential antioxidative and antiapoptotic defense of cancers to support their rapid growth [2,6]. Accordingly, we developed an antitumor strategy by targeting HO-1 in tumors. ZnPP thus became a good candidate for this treatment; however, its poor water-solubility greatly limits its application. To overcome this drawback, we previously developed a water-soluble ZnPP derivative, poly(ethylene glycol)-conjugated ZnPP (PEG–ZnPP), which showed remarkable antitumor effect with very less apparent side effects by selectively targeting tumor based on the EPR (Enhanced permeability and retention) effect [12,13].

Along this line, more recently we developed a micellar type of ZnPP by use of copolymer of styrene-maleic acid (SMA), namely SMA–ZnPP [14]. Similar to PEG–ZnPP, SMA–ZnPP exhibited good

☆ This work was partially supported by a Grant-in-Aid for Research (Nos. 17016076 and 22700927) on Cancer from the Ministry of Education, Culture, Sports and Science of Japan.

* Corresponding author. DDS Research Institute, Sojo University, Ikeda 4-22-1, Kumamoto 860-0082, Japan. Tel.: +81 96 326 4114; fax: +81 96 326 3158.
E-mail address: hirmaeda@ph.sojo-u.ac.jp (H. Maeda).
[1] These authors contributed equally to this paper.

0939-6411/$ - see front matter © 2012 Elsevier B.V. All rights reserved.
http://dx.doi.org/10.1016/j.ejpb.2012.04.016

water solubility, and it remained same HO inhibitory activity compared to native ZnPP. However, the loading of ZnPP in SMA–ZnPP micelle was much higher than that in PEG–ZnPP, which may substantially decrease the net weight of the compounds used for tumor therapy, thus reducing the viscosity of the injection solution and improve the therapeutic effectiveness/cost. Furthermore, from SMA–ZnPP micelle, free ZnPP was released at a constant rate of 20–30%/day. In addition, SMA–ZnPP micelle showed an apparent stoke's radius of 176.5 nm as measured by dynamic light scattering in a physiological solution [14]. It will further show a larger molecular size in circulation because of the albumin binding property of SMA [15,16]. Thus, the sustained in vivo antitumor effect was anticipated.

To investigate the therapeutic potential of SMA–ZnPP, in this study various tumor strains and normal cell lines were used to examine the pharmacological activity of SMA–ZnPP and the in vivo antitumor effect was evaluated by using various murine and rabbit tumor models. The intracellular uptake, pharmacokinetics and body distribution of SMA–ZnPP, and the safety were also investigated.

Table 1
IC_{50} of SMA–ZnPP against various tumor cells and normal cells.

Tumor cells	IC_{50} (μM)	Normal cells	IC_{50} (μM)
DLD-1	14.0	CV-1	50.0
Sk-Hep	16.0	HBE140	>50.0
HT-29	5.8	RLF	>200.0
A431	15.0	Hc	>50.0
KP-1N	3.6	HEK293	>50.0
CNE	19.4	CEF	25.2
ES2	9.8		
Lxc	4.2		
MCF-7	3.1		
Meth A	10.8		
B16/F10	20.1		
Mean	11.1 ± 1.9	Mean	>50.0

IC_{50} was determined by the MTT assay. See text for details.
DLD-1 and HT-29, human colon cancer cells; Sk-Hep, human liver cancer cell; A431, human lung cancer cell; CNE and Lxc, human laryngeal cancer cells; ES2, human ovarian cancer cell; KP-1N, human pancreatic cancer cell; MCF-7, human breast cancer cell; Meth A, mouse fibrosarcoma cell; B16/F10, mouse melanoma cell. CV1, monkey kidney fibroblast; HBE140, human bronchial epithelial cell; RLF, rat liver fibroblast; HEK293, human embryonic kidney cell; CEF, chick embryonic fibroblast; Hc, human hepatic cell.

2. Materials and methods

2.1. Materials

Protoporphrin IX was purchased from Sigma-Aldrich (St. Louis, MO). SMA with a mean molecular size of 1280 Da (Mw/Mn: 1.1) was obtained from Kuraray Ltd., Kurashiki, Japan. Other reagents were of commercial reagent grade and were used without further purification.

2.2. Animals

Female BALB/c mice and male C57BL/6 mice, 5–6 weeks of age and weighing 20–25 g, as well as New Zealand white rabbits about 3 months old, weighing 2.0–2.25 Kg, were from SLC, Inc. (Shizuoka, Japan). All experiments were carried out according to the guidelines of the Laboratory Protocol of Animal Handling, Sojo University.

2.3. Synthesis of SMA–ZnPP micelles

The preparation, purification and characterization of SMA–ZnPP micelle were described in our recent work [14].

2.4. In vitro cytotoxicity assay

In vitro cytotoxicity of SMA–ZnPP micelles was examined by use of MTT assay with 11 tumor cell lines and six normal cell lines as described in Table 1. Cells were plated in 96-well culture plates (3000 cells/well). After overnight pre-incubation, predetermined concentration of SMA–ZnPP was added to respective culture media, and the cells were further incubated for 72 h. Toxicity was quantified as the fraction of surviving cells relative to untreated controls.

2.5. Intracellular uptake of SMA–ZnPP

Intracellular uptake study was carried out in human laryngeal cancer cells Lxc. 50,000 cells were cultured in 16-well plates. After 12 h of culture, SMA–ZnPP solution in deionized water or free ZnPP, dissolved first in DMSO and then diluted with 0.01 M NaOH, were added to the cells at dose of 5 μM ZnPP equivalent. The medium containing drug was removed at predetermined time, and the cells were washed twice with PBS. Cells were then lysed by 1 ml lysis buffer (4 N HCl in 70% ethanol) then heated to 70 °C for 15 min. The solution was centrifuged at 15,000 rpm for 3 min, and the supernatant was used for measuring the fluorescence emission from 550 to 600 nm by excitation at 420 nm (corresponding to ZnPP) using a fluorescence spectroscopy (Hitachi F-4500, Tokyo, Japan). Experiments were also carried out in mouse fibrosarcoma Meth A cells and mouse melanoma B16/F10 cells similarly.

2.6. Pharmacokinetics of SMA–ZnPP after i.v. injection into tumor-bearing mice

In vivo pharmacokinetics of SMA–ZnPP was examined by the use of ^{65}Zn-radiolabeled derivatives. Radiolabeled SMA–ZnPP was prepared by the same method as that described by Iyer et al [14], in which ^{65}Zn-labeled zinc acetate (Riken, Saitama, Japan) was used.

Mouse sarcoma S180 cells (2×10^6) were implanted, s.c. in the dorsal skin of ddY mice. At 10–15 days after tumor inoculation when tumors reached a diameter of 7–10 mm, each mouse received i.v. injections of ^{65}Zn-labeled SMA–ZnPP via the tail vein [50 μg ZnPP equivalent, 45,000 cpm (0.75 kBq), 0.2 ml/injection]. After scheduled time, mice were killed, blood samples were drawn from the inferior vena cava, and mice were then subjected to reperfusion with 20 ml of physiological saline containing heparin (5 units/ml) to remove blood components in the blood vessels of the tissues. Then, tumor tissues as well as normal tissues, including the liver, the spleen, the kidney, the intestine, the heart, the lung, the brain and the muscle, were collected and weighed. Radioactivity of these tissues was measured by using a gamma counter (1480 WIZARD, Perkin Elmer, Waltham, MA).

The pharmacokinetics of SMA–ZnPP was also examined in Meth A and B16 tumor-bearing mice as described below, by measuring the fluorescence intensity at 590 nm of ZnPP. Namely, at schedule time after SMA–ZnPP (20 mg/kg, ZnPP equivalent) i.v. injection, mice were killed and each tissue and organ was resected. Each tissue was then weighted, and dimethylsulfoxide was added at a ratio of 1 mL/100 mg tissue, followed by homogenization to extract the SMA–ZnPP by centrifugation (12,000 g, 25 °C, 10 min) to precipitate the insoluble tissue debris. Content of SMA–ZnPP in the supernatant was quantified by fluorescent intensity (Ex. 422 nm, Em. 590 nm).

Please cite this article in press as: J. Fang et al., HSP32 (HO-1) inhibitor, copoly(styrene-maleic acid)-zinc protoporphyrin IX, a water-soluble micelle as anticancer agent: In vitro and in vivo anticancer effect, Eur. J. Pharm. Biopharm. (2012), http://dx.doi.org/10.1016/j.ejpb.2012.04.016

2.7. In vivo antitumor effect of SMA–ZnPP

Mouse Meth A fibrosarcoma and melanoma B16 were prepared by implanting Meth A and B16/F10 cells (2×10^6 cells) s.c. in the dorsal skin of BALB/c and C57BL/6 mice, respectively. On day 7–10 after tumor injection when tumors had reached a diameter of 5–7 mm, SMA–ZnPP micelles at the desired concentration were administered intravenously via the tail vein according to the treatment protocol. Growth of the tumors was monitored every 2 days by measuring tumor volume with a digital caliper, which was estimated by measuring longitudinal cross section (L) and transverse section (W) according to the formula $V = (L \times W^2)/2$.

VX-2 carcinoma that is a papilloma virus–induced squamous cell carcinoma was established in New Zealand white rabbits. Briefly, laparotomy was performed with central incision, using pentobarbital sodium for general anesthesia at dose of 30 mg/kg intravenously. A solid VX-2 tumor mass of about $2 \times 2 \times 2$ mm^3 was inoculated through forceps into the subcapsular parenchyma of left anterior lobe of the liver. Fourteen days after tumor inoculation, intravenous treatment with SMA–ZnPP (once a week) was commenced for successive 4 weeks. One month after treatment, another laparotomy was performed and the liver was exposed to measure the diameter of tumor. Three months after tumor inoculation, all survived animals were sacrificed, and liver biopsy from the tumor site was collected for histological examination.

2.8. Histological examination

Tissue specimens collected from VX-2 tumor models as described above were fixed with 10% buffered neutral formalin solution and were then embedded in paraffin. Sections were stained with H&E as usual.

2.9. Measurement of HO activity

Meth A, B16 and S180 tumor tissues, collected from tumor-bearing mice after 24 h with or without i.v. injection of SMA–ZnPP (20 mg/kg, ZnPP equivalent), were homogenized by a Polytron homogenization with ice-cold homogenate buffer [20 mM potassium phosphate buffer (pH 7.4) plus 250 mM sucrose, 2 mM EDTA, 2 mM phenylmethylsulfonyl fluoride, and 10 μg/ml leupeptin]. Homogenates were centrifuged at 10,000g for 30 min at 4 °C, after which the resultant supernatant was ultracentrifuged at 105,000g for 1 h at 4 °C. The microsomal fraction was suspended in 0.1 M potassium phosphate buffer (pH 7.4) followed by sonication for 2 s at 4 °C. The reaction mixture used for measuring HO activity composed of microsomal protein (1 mg), cytosolic fraction of rat liver (1 mg of protein) as a source of biliverdin reductase, 33 μM hemin and 333 μM NADPH in 1 ml of 90 mM potassium phosphate buffer (pH 7.4). The mixture was incubated for 15 min at 37 °C, and then, the reaction was terminated by the addition of 33 μl of 0.01 M HCl. The bilirubin formed in the reaction was extracted with 1 ml of chloroform, and the bilirubin concentration was determined spectrophotometrically by measuring the difference in absorbance between 465 and 530 nm, with a molar extinction coefficient of 40 mM^{-1} cm^{-1}.

2.10. Safety of SMA–ZnPP micelles

BALB/c mice with Meth A tumors of about 5–7 mm in diameter were used for this study. SMA–ZnPP micelles were administered at the dose of 50 mg/kg (ZnPP equivalent), which is 5–10 times higher concentration than therapeutic dose. Seventy-two hours later, mice were killed and blood samples were obtained. RBC, WBC counts and hemoglobin levels were determined by using an automated blood counter (F-800 Microcell Counter, Toa Medical Electronics, Kobe, Japan). Plasma obtained by centrifugation was used for measurement of enzyme activities of alanine aminotransferase, aspartate aminotransferase, lactate dehydrogenase, blood urea nitrogen and total creatine values by using a sequential multiple Auto Analyzer system (Hitachi Ltd., Tokyo, Japan).

2.11. Statistical analyses

All data were expressed as means ± SD. Student's t-test was used to compare differences between experimental groups, and it was considered statistically significant when $p < 0.05$.

3. Results

3.1. In vitro cytotoxicity of SMA–ZnPP

In human liver cancer Sk-Hep cells, SMA–ZnPP exhibited remarkable cytotoxicity, in a dose-dependent manner, whereas

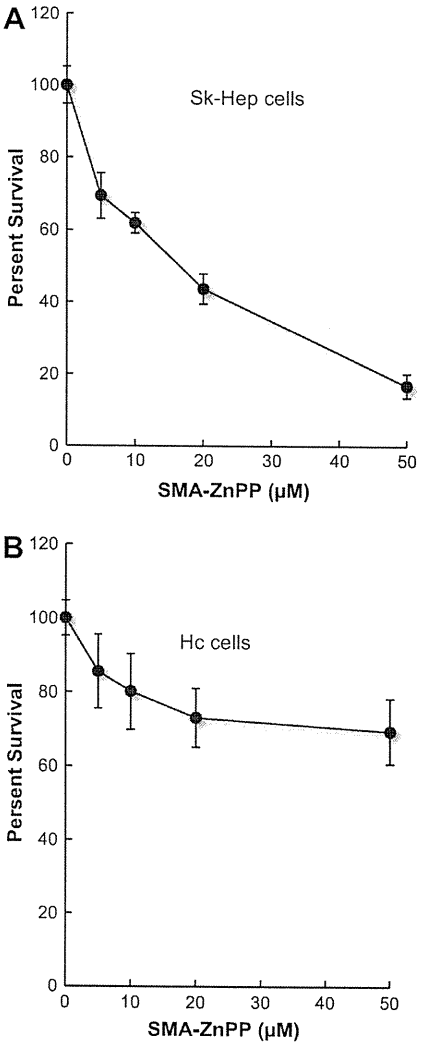

Fig. 1. In vitro cytotoxicity of SMA–ZnPP against normal (Hc) and tumor (Sk-Hep) cells. Cells were exposed to increasing concentration of SMA–ZnPP for 48 h, followed by MTT assay to determine cell viability. Values are mean ± SE (n = 6–8).

Please cite this article in press as: J. Fang et al., HSP32 (HO-1) inhibitor, copoly(styrene-maleic acid)-zinc protoporphyrin IX, a water-soluble micelle as anticancer agent: In vitro and in vivo anticancer effect, Eur. J. Pharm. Biopharm. (2012), http://dx.doi.org/10.1016/j.ejpb.2012.04.016

no significant cytotoxicity was observed up to 50 μM against normal hepatocytes Hc (Fig. 1 and Table 1). Similar results were found in other tumor and normal cell lines. The average 50% inhibitory concentration (IC_{50}) of SMA–ZnPP against different cells was summarized in Table 1. Most normal cells tested in this study exhibited relative tolerance to SMA–ZnPP treatment with IC_{50} of higher than 50 μM. In contrast, tumor cells showed much sensitive to this treatment, whose average IC_{50} was 11.1 ± 1.9 μM.

3.2. Intracellular uptake of SMA–ZnPP micelle

Fig. 2A shows a time-dependent internalization of SMA–ZnPP into Lxc cells, which is comparable to that of free ZnPP. These results suggest that the micellar formation of SMA did not impede the intracellular uptake of SMA–ZnPP. Instead, SMA–ZnPP appears more favorable than PEG–ZnPP micelles whose internalization was about 1/3 of that of SMA–ZnPP at 6 h after addition to the culture media (Fig. 2A). Similar results were obtained in Meth A (Fig. 2B) and B16/F10 cells (Fig 2C).

3.3. Pharmacokinetics and body distribution of SMA–ZnPP after i.v. injection

As shown in Fig. 3A, no significant prolonged plasma half-life ($t_{1/2}$) was observed for SMA–ZnPP. Namely, more than 50% of the SMA–ZnPP was removed from circulation during 10 min after i.v. injection. Moreover, no significant tumor accumulation of SMA–ZnPP was achieved, for example, the tumor concentration of SMA–ZnPP at 24 h after SMA–ZnPP administration was similar to those of most normal tissues (Fig. 3B).

However, surprisingly we found a remarkable increase in liver delivery of SMA–ZnPP, which is more than 20 times of that in plasma at 24 h after i.v. injection (Fig. 3A). Accumulation of SMA–ZnPP in liver tissue remained high for at least 4 days (Fig. 3A). Similar results were also observed in Meth A fibrosarcoma tumor and B16 melanoma tumor-bearing mice, respectively (Fig. S1). These findings suggested the potential application of SMA–ZnPP for cancers in the liver.

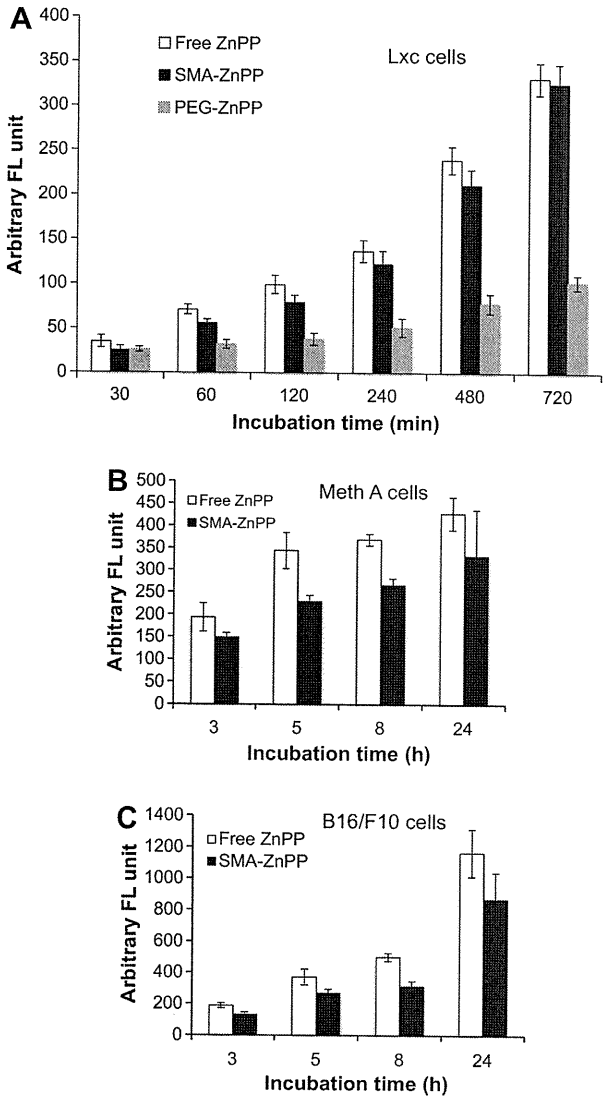

Fig. 2. Intracellular uptake of free ZnPP, SMA–ZnPP and PEG–ZnPP. Lxc cells (A), Meth A cells (B) and B16/F10 cells (C) were incubated with the investigated compounds at 5 μM (expressed in ZnPP equivalents) for different period of time. The amount of drug uptake by different tumor cells was determined measuring the fluorescence intensity after extracted from the cells, as described in Materials and Methods (2.5.). Values are mean ± SE ($n = 4$).

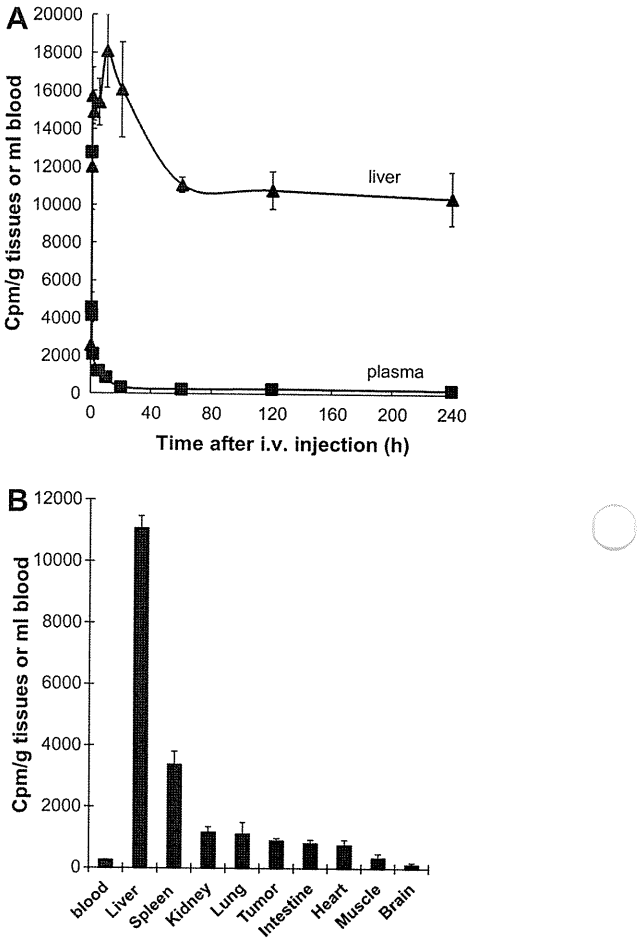

Fig. 3. Pharmacokinetics of SMA–ZnPP in ddY mice bearing Sarcoma 180 tumor as determined by using radioactive derivatives. Radiolabeled SMA–ZnPP was injected i.v. into tumor-bearing mice. After scheduled time periods, mice were killed, and samples of blood, tumor, liver and other normal tissues and organs were collected. Radioactivity of each tissue or organ was then measured. *A*, time-dependent change in SMA–ZnPP concentrations in plasma (■) and liver (▲). *B*, body distribution of SMA–ZnPP at 24 h after i.v. injection. Data are expressed as means; bars, ±SE ($n = 4$).

Please cite this article in press as: J. Fang et al., HSP32 (HO-1) inhibitor, copoly(styrene-maleic acid)-zinc protoporphyrin IX, a water-soluble micelle as anticancer agent: In vitro and in vivo anticancer effect, Eur. J. Pharm. Biopharm. (2012), http://dx.doi.org/10.1016/j.ejpb.2012.04.016

3.4. In vivo antitumor activity of SMA–ZnPP

Based on the findings of pharmacokinetics of SMA–ZnPP described in Fig. 3, we first investigated the in vivo antitumor effect of SMA–ZnPP in rabbit VX-2 tumor model transplanted in the liver. As shown in Fig. 4 and Table 2, a remarkable antitumor effect of SMA–ZnPP was observed. At 40 days after tumor transplantation, all of the non-drug treated control tumor-bearing rabbits died, whereas all animals receiving SMA–ZnPP did survive (Table 2). On days 60 and 80 after VX-2 tumor inoculation, when SMA–ZnPP was given at 4 and 8 mg/kg (ZnPP equivalent, weekly injection for 4 weeks), the survival rate was 60% and 80%, respectively, whereas 12 mg/kg resulted 100% survival on day 80 (Table 2). More important, histological examination showed that tumors became necrotic and fibrosis after SMA–ZnPP treatment (Fig. 4). In a long-term study, out of seven animals treated with 7 mg/kg weekly for 4 weeks, four animals were cured with no recurrence of the tumor of up to 2 years period of follow-up.

Further, the antitumor activity of SMA–ZnPP was examined in a Meth A mouse fibrosarcoma model. As shown in Fig. 5A, tumor growth was remarkably suppressed when SMA–ZnPP was administered at the dose of 4 mg/kg. Growth suppression continued to at least for 19 days after injection of SMA–ZnPP.

Table 2
Therapeutic effect of SMA–ZnPP on rabbit VX-2 papiloma implanted in the liver.

Group	Dose (mg/kg)[a]	% Survival after treatment[c]			Histological changes (by laparotomy)
		40 days[b]	60 days[b]	80 days[2]	
Control	0	0	0	0	Growing with invasion
SMA–ZnPP	4	100	60	60	Fibrosis appearing
	8	100	80	80	Necrosis, fibrosis in tumors
	12	100	100	100	Necrosis, totally fibrosis

See text and Fig. 4 for details.
[a] ZnPP equivalent. SMA–ZnPP was injected once weekly for 4 weeks at the indicated doses.
[b] Days after tumor inoculation.
[c] $n = 5–7$ Per group.

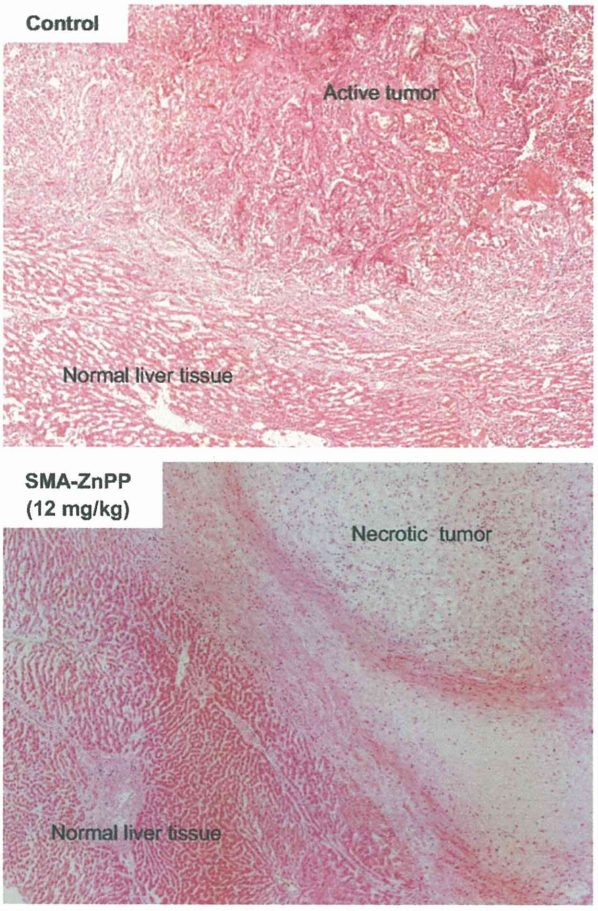

Fig. 4. Histological changes in rabbit VX-2 transplanted liver cancer after SMA–ZnPP treatment. Establishment of the tumor model is described in Materials and Methods. The dose of SMA–ZnPP was 12 mg/kg (ZnPP equivalent). Animals were killed, and tumor tissues were collected at 30 days (control group) and 60 days (SMA–ZnPP treatment group) after tumor inoculation, which were fixed by 10% buffered neutral formalin solution and were then subjected to H&E staining.

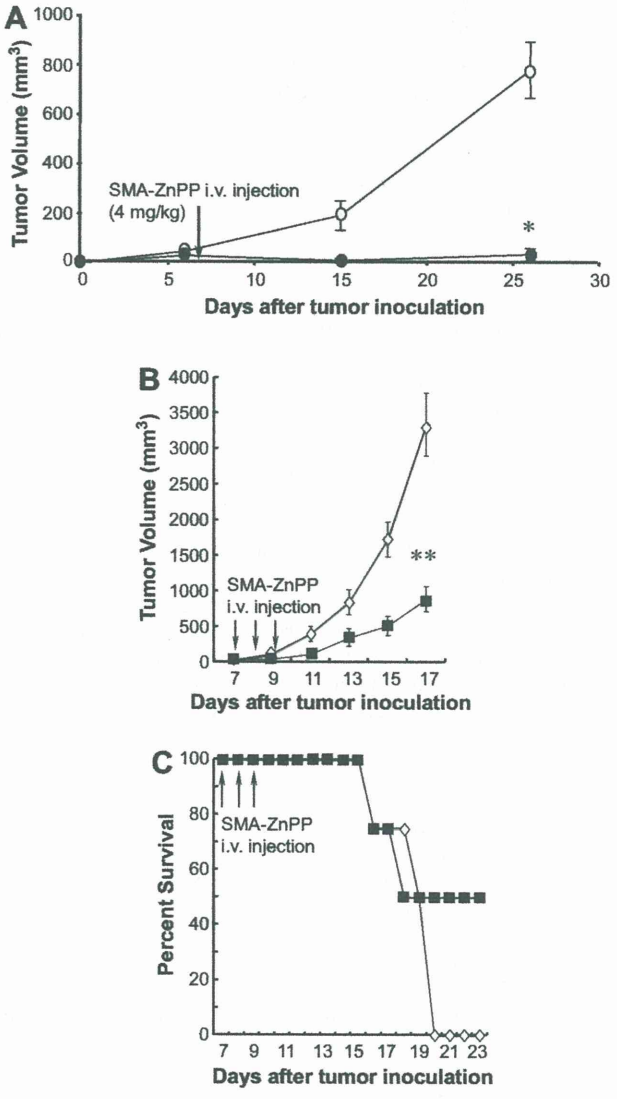

Fig. 5. *In vivo* antitumor effect of SMA–ZnPP. A shows the results in mouse MethA tumor model; ○, no drug control; ●, SMA–ZnPP (4 mg/kg ZnPP equivalent). B and C show the results of change in tumor size and survival of mouse B16 melanoma model; ◇, no drug control; ■, SMA–ZnPP (30 mg/kg ZnPP equivalent). Arrows indicate injections of SMA–ZnPP. Data are means ($n = 6–8$); bars, SE. *$P < 0.0001$; **$P < 0.001$, SMA–ZnPP treatment group vs untreated control group.

Similarly, in B16 melanoma in mice, which is known to progress rapidly and difficult to cure, significant suppression of tumor growth was found after 3 continuous injection of SMA–ZnPP at a

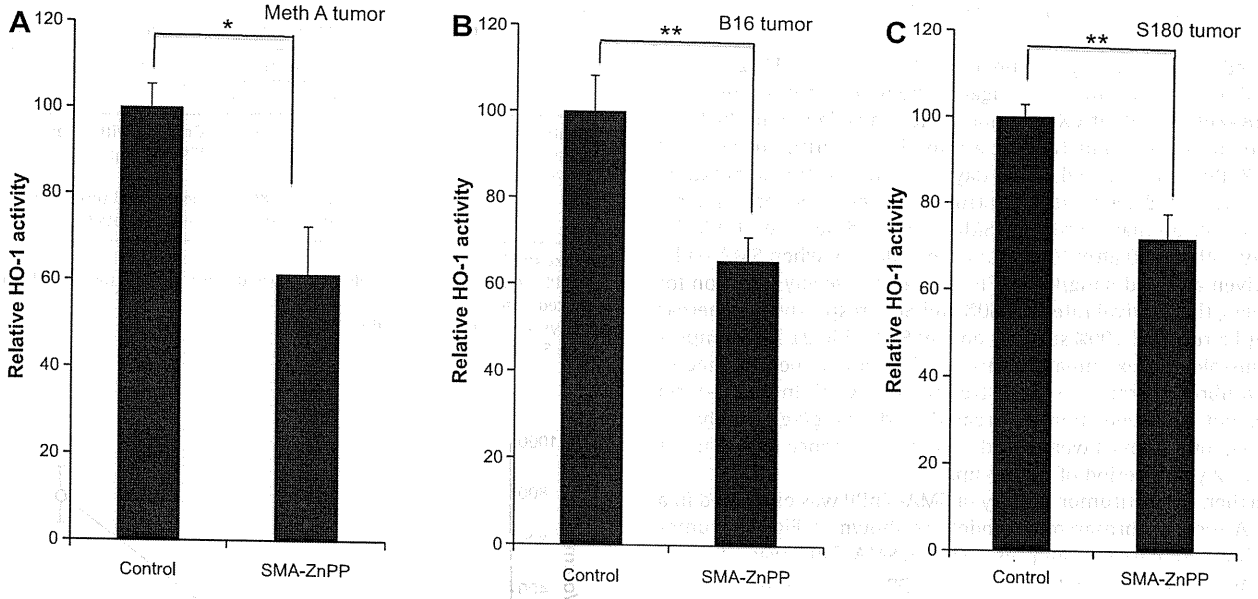

Fig. 6. Modulation by SMA–ZnPP of HO-1 activity in the Meth A (A), B16 (B) and S180 (C) solid tumor models. Tumor-bearing mice were i.v. injected with SMA–ZnPP (20 mg/kg, ZnPP equivalent). Twenty-four hours after the injection, tumors were obtained and were used for HO activity. Control mice values are means (n = 3–5); bars, SE. $^{*}P < 0.01$; $^{**}P < 0.005$, SMA–ZnPP treatment group vs untreated control group.

high dose (30 mg/kg) (Fig. 5B). Moreover, this treatment significantly contributed in the survival of tumor-bearing mice, that is, at 21 day after tumor inoculation, all mice of untreated control group died, whereas 50% of the mice in SMA–ZnPP treatment group remained alive (Fig. 5C).

3.5. Inhibition by SMA–ZnPP of HO activity in Meth A and B16 solid tumor

To clarify whether the in vivo suppression of tumor growth by SMA–ZnPP was due to the inhibition of HO activity, the enzyme activity of HO-1 in tumor after SMA–ZnPP treatment was examined. As shown in Fig. 6, HO-1 activity was significantly suppressed in all tested tumors (by 30–40%). These findings support our working hypothesis of the antitumor mechanisms of SMA–ZnPP, that is, through the HO-1 inhibition pathway, at least partly.

3.6. Adverse effect of SMA–ZnPP treatment

As summarized in Table 3, no significant adverse effects such as decreases in RBC and WBC counts and hemoglobin levels were found 72 h after SMA–ZnPP treatment at the dose of 50 mg/kg, which is much higher than the therapeutic dose or effective dose. Also, no significant changes in the liver enzymes and kidney functions were found under the same conditions (Table 3).

In addition, in a long-term follow-up of the above SMA–ZnPP treatment at high dose by a bolus administration (200 mg/kg), no death or body weight changes was observed up to 3 months after SMA–ZnPP injection (data not shown). These data strongly suggest the safety of SMA–ZnPP treatment.

4. Discussions

In this study, we demonstrated the superior and selective antitumor effect of SMA–ZnPP, both in vitro against various tumor cell lines (Fig. 1, Table 1), and in vivo against different type of solid tumors (Figs. 4 and 5), especially indicating its potential as a therapeutic for liver cancer. The antitumor activity of SMA–ZnPP is achieved by its targeting to the HO-1 that is a important "survival factor" of most tumors [2,5,6], which ZnPP is the pharmalogical active principle to inhibit HO-1 activity. This anticancer strategy was developed in our laboratory, and to improve the water-solubility and pharmacokinetics of ZnPP, micellar formations of ZnPP were developed by use of various water polymers, that is, PEG and SMA, both of which are widely used polymers to modify hardly soluble small molecular drugs.

One of the examples is PEG–ZnPP, which is a polymer conjugate that forms micelles in water solutions with superior in vivo pharmacokinetics [12,13]. Accordingly, it demonstrated a significant tumor growth suppression effect [13]. However, we have found a limitation to the use of PEG as polymeric carrier of ZnPP. Namely, PEG–ZnPP could only carry 1.5% ZnPP/PEG w/w ratio. This low loading of ZnPP in PEG conjugate requires relatively large injection dose that leads to high viscosity at higher dose that may be needed

Table 3
Effect of SMA–ZnPP in hematology and liver, kidney function.[a]

	Hematological findings			Kidney function		Liver enzymes		
	RBC (10^4/μl)	WBC (/μl)	Hb (g/l)	BUN (mg/dl)	Cr (mg/dl)	AST (IU/l)	ALT (IU/l)	LDH (IU/l)
Control	868.7 ± 60.6	186.7 ± 18.8	13.4 ± 1.2	23.0 ± 0.6	0.11 ± 0.01	395.3 ± 91.8	26.0 ± 3.8	10697.5 ± 2247.6
SMA–ZnPP[b]	820.0 ± 70.5	206.5 ± 52.0	2.3 ± 1.2	25.9 ± 1.1	0.13 ± 0.01	351.8 ± 88.9	27.5 ± 2.7	9755.0 ± 1570.8

Abbreviations used are: Hb, hemoglobin; BUN, blood urea nitrogen; Cr, creatinine; AST, aspartate aminotransferase; ALT, alanine aminotransferase; LDH, lactate dehydrogenase.

[a] No significant difference was found between SMA–ZnPP treatment group and control group in all selected indices. Values are presented as means ± SE.

[b] SMA–ZnPP was administered i.v. at 50 mg/kg (ZnPP equivalent). Assays were carried out at 72 h after SMA–ZnPP treatment.

Please cite this article in press as: J. Fang et al., HSP32 (HO-1) inhibitor, copoly(styrene-maleic acid)-zinc protoporphyrin IX, a water-soluble micelle as anticancer agent: In vitro and in vivo anticancer effect, Eur. J. Pharm. Biopharm. (2012), http://dx.doi.org/10.1016/j.ejpb.2012.04.016

for possible human therapeutic application. Further, the cost of expensive PEG for such low loading drug results in relatively high drug cost, which will become a social problem. To overcome these drawbacks, we further developed a micellar type of ZnPP using SMA, namely SMA–ZnPP, which can achieve higher loading of 15–45% w/w [14]. The high loading did not affect its solubility in this micelle; on the contrary, it resulted in solubility of up to 150 mg/ml, which can exceed the solubility required for therapeutic application.

In addition to the increased water-solubility, SMA–ZnPP also showed faster cellular uptake in all three different tumor cell lines tested, which is comparable to that of free ZnPP. Namely, it was about three times higher than PEG–ZnPP (Fig. 2). In our recent report, we compared the intracellular fate of free ZnPP and its polymer conjugates and micells (i.e., SMA–ZnPP and PEG–ZnPP) [17]. While free ZnPP was taken up via free diffusion, SMA–ZnPP was mostly internalized by endocytosis. During this internalization process, the micelle integrity was disrupted and free ZnPP appeared to be released upon internalization with cell membrane components [17]. However, the intracellular uptake of PEG–ZnPP was greatly impeded, which is called PEG dilemma [17,18]. The data in present study are consistent with our previous findings, suggesting that SMA–ZnPP shows stronger cytotoxicity than PEG–ZnPP because of its efficient cell uptake. To verify this notion, we tested the cytotoxicity of SMA–ZnPP in various tumor cells, which exhibited a mean IC_{50} of 11.1 μM (Table 1), whereas as reported previously, PEG–ZnPP showed a relatively higher IC_{50} of about 20 μM [13].

SMA–ZnPP micelle appeared as large molecule with the apparent molecular size of 144 kDa as determined by size exclusion chromatography [14]. As such large molecule, we thus anticipated its higher intratumor concentration based on the EPR effect followed by rapid endocytosis. It appears to be an universal phenomenon of macromolecular drugs with molecular weight larger than 40 kDa, a feature of the EPR effect, which they are selectively accumulated and being retained in solid tumor because of the unique anatomical and pathophysiological characteristics of tumor vasculature [19], and it is now known as a gold standard for the design and development of anticancer drugs [20–26].

However, we could not find good EPR effect for SMA–ZnPP in the present study, even tough it showed stable macromolecular micellar structure in physiological solution as described in our previous report [14]. This may be probably due to the lack of in vivo stability particularly in circulation, namely SMA–ZnPP micelle may be disrupted during circulation or upon uptake by RES which are rich in liver and spleen. Because of the high affinity to liver and spleen, free ZnPP released from SMA–ZnPP after disruption will accumulate mostly in liver and spleen. In consistent with this notion, we found interestingly that SMA–ZnPP significantly accumulated in liver tissue, for example, 20 times higher than plasma concentration at 24 h after i.v. injection, and it retained in the liver tissue at relatively high concentration for more than 96 h (Fig. 3C). The disruption and high liver accumulation of SMA–ZnPP could be improved by conjugation of SMA with ZnPP via a convalent amide bond (unpublished data). These data of distribution study, however, strongly suggest us to use SMA–ZnPP for the treatment of the liver cancer that is very difficult to treat in clinic with high mortality. Accordingly, in the present study, a significant cure rate of rabbits with VX-2 tumor implanted in the liver was achieved by using SMA–ZnPP, evidences being not only by the survival rate of animals, but also by the histopathological examination, that is, SMA–ZnPP treatment resulted in more necrosis as well as fibrosis of tumor tissues (Fig. 4 and Table 2).

Moreover, in other tumor models, that is, Meth A and B16 melanoma, SMA–ZnPP markedly reduced the tumor volume (Fig. 5), though complete regression of the tumor was not possible in B16 melanoma as in VX-2. In addition, compared to B16 tumors, Meth A tumors showed higher sensitivity to this treatment. Namely, a lower dose of SMA–ZnPP (at 4 mg/kg bolus i.v.) exhibited relatively remarkable tumor suppression effect (Fig. 5A) compared to B16 tumor with higher dose treatment of SMA–ZnPP (three injections of 30 mg/kg) (Fig. 5B). These findings are consistent with the cytotoxicity data of these two cell lines (IC_{50} of Meth A, 10.8 μM vs 20.1 μM of B16, Table 1).

The antitumor mechanisms of SMA–ZnPP were considered mostly due to the HO inhibition activity, and variation of HO-1 dependence susceptibility in different tumors may result in the variation of therapeutic effect. This notion was partly verified in the present study, namely, SMA–ZnPP treatment decreased the HO-1 activity in Meth A, B16 and S180 solid tumors, significantly though not largely (Fig. 6). It should be also noted that many other possible mechanisms may also work for the antitumor activity of SMA–ZnPP. For example, it has been reported that ZnPP-induced apoptosis of hamster fibroblasts by upregulating p53 expression, through ZnPP-mediated Egr-1 binding [27]. More recently, down-regulation of BCR/ABL oncogene by ZnPP in case of chronic myeloid leukemia (CML) has been reported [28]. Administration of PEG–ZnPP or SMA–ZnPP showed a remarkable therapeutic potential against CML [29,30], even imatinib-resistant CML [31]. In addition, SMA copolymer itself was found to have an active role in endogenous interferon induction as well as the activation of NK cells [32–34]. Furthermore, zinc is also known as an essential messenger molecule in stimulating immune response [35], and it was also used for the treatment of prostate cancer, probably via a mitochondrial-mediated apoptotic pathway [36–38]; it thus may serve as another mechanism of SMA–ZnPP-induced antitumor effect by releasing zinc from the porphyrin ring of ZnPP. The roles of various factors in mediating different anticancer activity of SMA–ZnPP in tumors, however, remain to be investigated.

Even though SMA–ZnPP accumulated predominantly in the liver tissues, we did not find apparent adverse effects during our experiments. In addition, no deterioration of the liver functions was observed even at high dose of SMA–ZnPP (50 mg/kg) (Table 3). This may be, at least partly, due to the differences of sensitivities to SMA–ZnPP between normal and tumor cells. This notion was supported by in vitro MTT assay, which showed a relatively strong cytotoxicity of SMA–ZnPP against various tumor cells (Table 1), that is, the IC_{50} of SMA–ZnPP to human liver cancer cells Sk-Hep was 16 μM, and the range of IC_{50} in different tumor cells was between 3 and 20 μM. Importantly and interestingly, normal cells seemed to be much tolerant to SMA–ZnPP. Namely, the IC_{50} of SMA–ZnPP to normal hepatocytes Hc was higher than 50 μM, as well as other normal cells (Table 1). The difference of the responses of tumor cells and normal cells against SMA–ZnPP treatment may be due to the difference of HO-1 expression between tumor and normal cells, as described earlier [2,5,6,13]; however, further investigations are needed to define this correlation.

SMA–ZnPP used in our animal study, with some exceptions, was at the dose range of 1–10 mg/kg; however, animals were able to tolerate as high as 50 mg/kg without any apparent toxicity as reflected by blood cells count and biochemical examination of liver and kidney functions (Table 3), as well as survival rate. These data indicate the high safety of SMA–ZnPP with a wide therapeutic window.

5. Conclusions

The water-soluble micellar type of HO-1 inhibitor SMA–ZnPP was found to be effective in many solid tumor models, especially VX-2 tumor transplanted in the liver of rabbit. The drug accumulated in the liver was very high, while clearance from the circula-

Please cite this article in press as: J. Fang et al., HSP32 (HO-1) inhibitor, copoly(styrene-maleic acid)-zinc protoporphyrin IX, a water-soluble micelle as anticancer agent: In vitro and in vivo anticancer effect, Eur. J. Pharm. Biopharm. (2012), http://dx.doi.org/10.1016/j.ejpb.2012.04.016

tion was relatively rapid. SMA–ZnPP was examined both in vitro and in vivo; whereas it showed relatively potent cytotoxicity to tumor cells (average IC_{50} of about 11 μM); the IC_{50} of normal cells was higher than 50 μM, which resulted in very little adverse effects to tumor-bearing animals. These findings suggest the potential use of SMA–ZnPP as a novel anticancer drug especially for liver cancer, which warrants further development and investigation.

Acknowledgment

The authors wish to thank Dr. Takahiro Seki for excellent technical assistance.

Appendix A. Supplementary material

Supplementary data associated with this article can be found, in the online version, at http://dx.doi.org/10.1016/j.ejpb.2012.04.016.

References

[1] M.D. Maines, Heme oxygenase: function, multiplicity, regulatory mechanisms, and clinical applications, FASEB J. 2 (1988) 2257–2268.
[2] J. Fang, T. Akaike, H. Maeda, Antiapoptotic role of heme oxygenase (HO) and the potential of HO as a target in anticancer treatment, Apoptosis 9 (2004) 27–35.
[3] S.M. Keyse, R.M. Tyrrell, Heme oxygenase is the major 32-kDa stress protein induced in human skin fibroblasts by UVA radiation, hydrogen peroxide, and sodium arsenite, Proc. Natl. Acad. Aci. USA 86 (1989) 99–103.
[4] R. Motterlini, R. Foresti, R. Bassi, B. Calabrese, J.E. Clark, C.J. Green, Endothelial heme oxygenase-1 induction by hypoxia. Modulation by inducible nitric oxide synthase and S-nitrosothiols, J. Biol. Chem. 275 (2000) 13613–13620.
[5] K. Doi, T. Akaike, S. Fujii, S. Tanaka, N. Ikebe, T. Beppu, S. Shibahara, M. Ogawa, H. Maeda, Induction of haem oxygenase-1 by nitric oxide and ischaemia in experimental solid tumours and implications for tumour growth, Br. J. Cancer 80 (1999) 1945–1954.
[6] S. Tanaka, T. Akaike, J. Fang, T. Beppu, M. Ogawa, F. Tamura, Y. Miyamoto, H. Maeda, Antiapoptotic effect of haem oxygenase-1 induced by nitric oxid' in experimental solid tumour, Br. J. Cancer 88 (2003) 902–909.
[7] J.P. Greenstein, Biochemistry of Cancer, second ed., Academic Press, New ' rk, 1954.
[8] Y. Hasegawa, T. Takano, A. Miyauchi, F. Matsuzaka, H. Yoshida, K. Kuma, N. Amino, Decreased expression of glutathione peroxidase mRNA in thyroid anaplastic carcinoma, Cancer Lett. 182 (2002) 69–74.
[9] N. Yamanaka, D. Deamer, Superoxide dismutase activity in WI-38 cell cultures: effect of age, trypsinization and SV-40 transformation, Physiol. Chem. Phu.. ' (1974) 95–106.
[10] K. Sato, K. Ito, H. Kohara, Y. Yamaguchi, K. Adachi, H. Endo, Negative regulation of catalase gene expression in hepatoma cells, Mol. Cell. Biol. 12 (1992) 2525–2533.
[11] J. Fang, D. Deng, H. Nakamura, T. Akuta, H. Qin, A.K. Iyer, K. Greish, H. Maeda, Oxystress inducing antitumor therapeutics via tumor-targeted delivery of PEG-conjugated D-amino acid oxidase, Int. J. Cancer 122 (2008) 1135–1144.
[12] S.K. Sahoo, T. Sawa, J. Fang, S. Tanaka, Y. Miyamoto, T. Akaike, H. Maeda, Pegylated zinc protoporphyrin: a water-soluble heme oxygenase inhibitor with tumor-targeting capacity, Bioconjug. Chem. 13 (2002) 1031–1038.
[13] J. Fang, T. Sawa, T. Akaike, T. Akuta, S.K. Sahoo, G. Khaled, A. Hamada, H. Maeda, In vivo antitumor activity of pegylated zinc protoporphyrin: targeted inhibition of heme oxygenase in solid tumor, Cancer Res. 63 (2003) 3567–3574.
[14] A.K. Iyer, K. Greish, J. Fang, R. Murakami, H. Maeda, High-loading nanosized micelles of copoly(styrene-maleic acid)–zinc protoporphyrin for targeted delivery of a potent heme oxygenase inhibitor, Biomaterials 28 (2007) 1871–1881.
[15] A. Kobayashi, T. Oda, H. Maeda, Protein binding of macromolecular anticancer agent SMANCS: characterization of poly(styrene-co-maleic acid) derivatives as an albumin binding ligand, J. Bioact. Compat. Polym. 3 (1988) 319–333.
[16] K. Greish, A. Nagamitsu, J. Fang, H. Maeda, Copoly(styrene-maleic acid)–pirarubicin micelles: high tumor-targeting efficiency with little toxicity, Bioconjug. Chem. 16 (2005) 230–236.
[17] H. Nakamura, J. Fang, B. Gahininath, K. Tsukigawa, H. Maeda, Intracellular uptake and behavior of two types zinc protoporphyrin (ZnPP) micelles, SMA–ZnPP and PEG–ZnPP as anticancer agents; unique intracellular disintegration of SMA micelles, J. Control. Release 155 (2011) 367–375.
[18] H. Hatakeyama, H. Akita, H. Harashima, A multifunctional envelope type nano device (MEND) for gene delivery to tumours based on the EPR effect: a strategy for overcoming the PEG dilemma, Adv. Drug Deliv. Rev. 63 (2011) 152–160.
[19] Y. Matsumura, H. Maeda, A new concept for macromolecular therapeutics in cancer chemotherapy: mechanism of tumoritropic accumulation of proteins and the antitumor agent SMANCS, Cancer Res. 46 (1986) 6387–6392.
[20] H. Maeda, T. Sawa, T. Konno, Mechanism of tumor-targeted delivery of macromolecular drugs, including the EPR effect in solid tumor and clinical overview of the prototype polymeric drug SMANCS, J. Control. Release 74 (2001) 47–61.
[21] K. Greish, J. Fang, T. Inutsuka, A. Nagamitsu, H. Maeda, Macromolecular therapeutics: advantages and prospects with special emphasis on solid tumour targeting, Clin. Pharmacokinet. 42 (2003) 1089–1105.
[22] H. Maeda, Tumor-selective delivery of macromolecular drugs via the EPR effect: background and future prospects, Bioconjug. Chem. 21 (2010) 797–802.
[23] R. Duncan, The dawning era of polymer therapeutics, Nat. Rev. Drug Discov. 2 (2003) 347–360.
[24] H. Maeda, G.Y. Bharate, J. Daruwalla, Polymeric drugs for efficient tumor-targeted drug delivery based on EPR-effect, Eur. J. Pharm. Biopharm. 71 (2009) 409–419.
[25] T. Seki, J. Fang, H. Maeda, Tumor targeted macromolecular drug delivery based on the enhanced permeability and retention effect in solid tumor, in: Y. Lu, R.I. Mahato (Eds.), Pharmaceutical Perspectives of Cancer Therapeutics, AAPS-Springer Publishing, New York, 2009, pp. 93–102.
[26] J. Fang, H. Nakamura, H. Maeda, The EPR effect: unique features of tumor blood vessels for drug delivery, factors involved, and limitations and augmentation of the effect, Adv. Drug Deliv. Rev. 63 (2010) 136–151.
[27] G. Yang, X. Nguyen, J. Qu, P. Rekulapelli, D.K. Stevenson, P.A. Dennery, Unique effects of zinc protoporphyrin on HO-1 induction and apoptosis, Blood 97 (2001) 1306–1313.
[28] M. Mayerhofer, S. Florian, M.T. Krauth, K.J. Aichberger, M. Bilban, R. Marculescu, D. Printz, G. Fritsch, O. Wagner, E. Selzer, W.R. Sperr, P. Valent, C. Sillaber, Identification of heme oxygenase-1 as a novel BCR/ABL-dependent survival factor in chronic myeloid leukemia, Cancer Res. 64 (2004) 3148–3154.
[29] R. Kondo, K.V. Gleixner, M. Mayerhofer, A. Vales, A. Gruze, P. Samorapoompichit, K. Greish, M.T. Krauth, K.J. Aichberger, W.F. Pickl, H. Esterbauer, C. Sillaber, H. Maeda, P. Valent, Identification of heat shock protein 32 (Hsp32) as a novel survival factor and therapeutic target in neoplastic mast cells, Blood 110 (2007) 661–669.
[30] E. Hadzijusufovic, L. Rebuzzi, K.V. Gleixner, V. Ferenc, B. Peter, R. Kondo, A. Gruze, M. Kneidinger, M.T. Krauth, M. Mayerhofer, P. Samorapoompichit, K. Greish, A.K. Iyer, W.F. Pickl, H. Maeda, M. Willmann, P. Valent, Targeting of heat-shock protein 32/heme oxygenase-1 in canine mastocytoma cells is associated with reduced growth and induction of apoptosis, Exp. Hematol. 36 (2008) 1461–1470.
[31] M. Mayerhofer, K.V. Gleixner, J. Mayerhofer, G. Hoermann, E. Jaeger, K.J. Aichberger, R.G. Ott, K. Greish, H. Nakamura, S. Derdak, P. Samorapoompichit, W.F. Pickl, V. Sexl, H. Esterbauer, I. Schwarzinger, C. Sillaber, H. Maeda, P. Valent, Targeting of heat shock protein 32 (Hsp32)/heme oxygenase-1 (HO-1) in leukemic cells in chronic myeloid leukemia: a novel approach to overcome resistance against imatinib, Blood 111 (2008) 2200–2210.
[32] F. Suzuki, R.B. Pollard, S. Uchimura, T. Munakata, H. Maeda, Role of natural killer cells and macrophages in the nonspecific resistance to tumors in mice stimulated with SMANCS, a polymer-conjugated derivative of neocarzinostatin, Cancer Res. 50 (1990) 3897–3904.
[33] F. Suzuki, T. Munakata, H. Maeda, Interferon induction by SMANCS: a polymer-conjugated derivative of neocarzinostatin, Anticancer Res. 8 (1988) 97–103.
[34] T. Oda, T. Morinaga, H. Maeda, Stimulation of macrophage by polyanions and its conjugated proteins and effect on cell membrane, Proc. Soc. Exp. Biol. Med. 181 (1986) 9–17.
[35] H. Haase, J.L. Ober-Blöbaum, G. Engelhardt, S. Hebel, A. Heit, H. Heine, L. Rink, Zinc signals are essential for lipopolysaccharide-induced signal transduction in monocytes, J. Immunol. 181 (2008) 6491–6502.
[36] L.C. Costello, R.B. Franklin, P. Feng, Mitochondrial function, zinc, and intermediary metabolism relationships in normal prostate and prostate cancer, Mitochondrion 5 (2005) 143–153.
[37] P. Feng, T. Li, Z. Guan, R.B. Franklin, L.C. Costello, The involvement of Bax in zinc-induced mitochondrial apoptogenesis in malignant prostate cells, Mol. Cancer 7 (2008) 25.
[38] S.F. Lin, H. Wei, D. Maeder, R.B. Franklin, P. Feng, Profiling of zinc-altered gene expression in human prostate normal vs. cancer cells: a time course study, J. Nutr. Biochem. 20 (2009) 1000–1012.

Please cite this article in press as: J. Fang et al., HSP32 (HO-1) inhibitor, copoly(styrene-maleic acid)-zinc protoporphyrin IX, a water-soluble micelle as anticancer agent: In vitro and in vivo anticancer effect, Eur. J. Pharm. Biopharm. (2012), http://dx.doi.org/10.1016/j.ejpb.2012.04.016